Temporal and Spatial Variation in Peatland Carbon Cycling and Implications for Interpreting Responses of an Ecosystem-Scale Warming Experiment

Natalie A. Griffiths*
Paul J. Hanson
Daniel M. Ricciuto
Colleen M. Iversen
Climate Change Science Inst. and
    Environmental Sciences Division
Oak Ridge National Lab.
Oak Ridge, TN 37831

Anna M. Jensen
Climate Change Science Inst. and
    Environmental Sciences Division
Oak Ridge National Lab.
Oak Ridge, TN 37831

current address,
Dep. of Forestry and Wood Technology
Linnaeus Univ.
Växjö,
Sweden

Avni Malhotra
Climate Change Science Inst. and
    Environmental Sciences Division
Oak Ridge National Lab.
Oak Ridge, TN 37831

Karis J. McFarlane
Center for Accelerator Mass
    Spectrometry
Lawrence Livermore National Lab.,
Livermore, CA 94550

Richard J. Norby
Climate Change Science Inst. and
    Environmental Sciences Division
Oak Ridge National Lab.
Oak Ridge, TN 37831

Khachik Sargsyan
Sandia National Laboratories
Livermore, CA 94551

Stephen D. Sebestyen
Northern Research Station
USDA Forest Service
Grand Rapids, MN 55744

Xiaoying Shi
Anthony P. Walker
Eric J. Ward
Jeffrey M. Warren
Climate Change Science Inst. and
    Environmental Sciences Division
Oak Ridge National Lab.
Oak Ridge, TN 37831

David J. Weston
Climate Change Science Inst.
    and Biosciences Division
Oak Ridge National Lab.
Oak Ridge, TN 37831

Core Ideas

- **We compared spatial vs. temporal variation in C cycle processes and drivers in a bog.**

- **The bog was indistinguishable as a C source or sink because of high spatial variation.**

- **Sensitive C cycle parameters in the model differed under ambient vs. warming scenarios.**

- **Characterizing pretreatment variability is necessary when interpreting warming effects.**

Abbreviations: ELM_SPRUCE; SPRUCE-specific version of the Energy Exascale Earth System model; ANPP, aboveground net primary production; CI, confidence interval; [CO_2], CO_2 concentration; DOC, dissolved organic C; flnr, fraction of leaf N in ribulose-1,5-biphosphate carboxylase/oxygenase; NEE, net ecosystem exchange; NEP, net ecosystem production; NPP, net primary production; PFT, plant functional type; SPRUCE, Spruce and Peatland Responses Under Changing Environments project; TOC, total organic C.

We are conducting a large-scale, long-term climate change response experiment in an ombrotrophic peat bog in Minnesota to evaluate the effects of warming and elevated CO_2 on ecosystem processes using empirical and modeling approaches. To better frame future assessments of peatland responses to climate change, we characterized and compared spatial vs. temporal variation in measured C cycle processes and their environmental drivers. We also conducted a sensitivity analysis of a peatland C model to identify how variation in ecosystem parameters contributes to model prediction uncertainty. High spatial variability in C cycle processes resulted in the inability to determine if the bog was a C source or sink, as the 95% confidence interval ranged from a source of 50 g C m^{-2} yr^{-1} to a sink of 67 g C m^{-2} yr^{-1}. Model sensitivity analysis also identified that spatial variation in tree and shrub photosynthesis, allocation characteristics, and maintenance respiration all contributed to large variations in the pretreatment estimates of net C balance. Variation in ecosystem processes can be more thoroughly characterized if more measurements are collected for parameters that are highly variable over space and time, and especially if those measurements encompass environmental gradients that may be driving the spatial and temporal variation (e.g., hummock vs. hollow microtopographies, and wet vs. dry years). Together, the coupled modeling and empirical approaches indicate that variability in C cycle processes and their drivers must be taken into account when interpreting the significance of experimental warming and elevated CO_2 treatments.

Peatland ecosystems accumulate and store a disproportionately large amount of C in organic soils relative to their global areal coverage. Northern peatlands store an estimated 500 ± 100 Pg C (Yu, 2012); however, there is wide variation in published estimates (125–621 Pg C) (summarized in Yu, 2012). Estimates of C accumulation rates in northern peatlands are also variable, and range from 8 to 38 g C m^{-2} yr^{-1} (Gorham, 1991, 1995; Turunen et al., 2002; Yu et al., 2010; Loisel et al., 2014). Part of the variability in estimated peatland C stocks and accumulation rates reflects the general lack of data on peat depth, bulk density, and C content, and underrepresentation of certain northern peatland areas (Yu, 2012). Further, most C stock and accumulation rate estimates are based on data from one peat core per peatland, despite known within-peatland variability, as determined from multiple cores (Korhola et al., 1996; Ohlson and Økland, 1998; Roulet et al., 2007; van Bellen et al., 2011; K.J. McFarlane, unpublished data). For example, C accumulation rates from 48 cores collected in a *Sphagnum*-dominated bog in Norway varied from 26 to 454 g C m^{-2} yr^{-1} (Ohlson and Økland, 1998).

Contemporary C flux estimates from peatlands can also vary because of the lack of data over large temporal and spatial scales and the variety of methodologies used to measure the different components of net ecosystem C balance (Roulet et al., 2007; Yu, 2012). Although net CO_2 flux is often the largest component of net ecosystem C balance in peatlands (Limpens et al., 2008; Yu, 2012), C losses via CH_4 efflux and dissolved organic C (DOC) in stream flow can be substantial contributors to overall net C balance estimates (Limpens et al., 2008); however, CH_4 and DOC fluxes are often not measured. For example, if CH_4 and DOC fluxes had not been included in the calculation of net C flux for Mer Bleue bog (Ontario, Canada), peatland C uptake would have been overestimated by 40 to 80% (Roulet et al., 2007).

Net C flux is the balance between ecosystem production and respiration, which depends, in large part, on how *Sphagnum*, other mosses, and vascular plants (herbs, grasses, shrubs, and trees) respond to the prevailing environmental conditions (e.g., microtopography, nutrient availability, precipitation, and temperature). Therefore, C fluxes can vary across different peatlands because of variation in environmental characteristics and geographical settings. Net ecosystem exchange (NEE) of CO_2 is typically less variable than CH_4 emissions across peatlands (Limpens et al., 2008), with variation in CH_4 emissions being strongly affected by water table level fluctuations (Bubier et al., 2005). Studies that have measured contemporary C fluxes for at least 2 yr have also demonstrated variation in annual C fluxes across different peatlands (Roulet et al., 2007; Nilsson et al., 2008; Dinsmore et al., 2010; Koehler et al., 2011; Olefeldt et al., 2012; summarized in Yu, 2012); net C flux rates range from a C sink of 101 g C m^{-2} yr^{-1} at Auchencorth Moss in Scotland (Dinsmore et al., 2010) to a C source of 13.8 g C m^{-2} yr^{-1} at Mer Bleue (Roulet et al., 2007).

Within a peatland, C cycling can also vary across multiple spatial and temporal scales. For example, at the microtopographic scale (i.e., hummocks and hollows), CH_4 emission is higher and CO_2 uptake is lower in wetter, lower-relief hollows than in drier, higher-relief hummocks (Bubier et al., 1993; Waddington and Roulet, 1996; Dise et al., 2011; Dorodnikov et al., 2013). Carbon fluxes also vary at larger spatial scales within a peatland. For example, in temperate peatlands with lagg margins, net CH_4 emissions can be higher in the wetter margins than in the drier center (Crill et al., 1988). Although C fluxes can vary across different spatial scales in a peatland, these C cycling processes also vary at multiple temporal scales. Interannual variation in net C flux in a peatland can be substantial and largely driven by hydrology (Shurpali et al., 1995; Waddington and Roulet, 1996, 2000; Roulet et al., 2007; Dise et al., 2011). For instance, a peatland in north-central Minnesota was a C source of 71 g C m^{-2} yr^{-1} in a dry year and a C sink of 32 g C m^{-2} yr^{-1} in a wet year (Shurpali et al., 1995). Seasonal patterns in C flux can also vary across spatial scales. For example, the onset of thaw in a peatland complex in Manitoba, Canada, differentially affected the timing of when hummocks and hollows switched from being C sources to C sinks (Bubier et al., 1998). Prior to snowmelt, hummocks and hollows were both C sources. After the peat surface thawed, hummocks became C sinks but hollows were C sources for another 3 wk until the ice thawed in these locations (Bubier et al., 1998).

Quantifying the variability in peatland C cycling is necessary for understanding historical and current C dynamics and for developing a predictive understanding of the climate system. Most global C cycle models have an incomplete representation of peatland processes, which contributes to large discrepancies among global estimates of terrestrial C storage (Tian et al., 2015). Although such models are being evaluated against peatland observations (e.g., Sulman et al., 2012; Melton et al., 2013), relatively little has been done to synthesize observed spatial variability and measurement uncertainties in peatlands, or in understanding the drivers of model uncertainty. In modeling frameworks, variations in peatland C stocks and fluxes are caused by differences in environmental drivers, boundary conditions, and model parameters. Model ensembles can be performed to estimate prediction uncertainties and to perform parameter sensitivity analysis. Sensitivity analysis can investigate which parameters and related processes are the most significant contributors to these variations. Sensitivity analysis has been applied in a number of global C cycle models and has identified a small number of critical parameters with relatively large impacts on uncertainty, especially the parameters associated with photosynthesis, respiration, and plant allocation processes (e.g., Dietze et al., 2014; Lu et al., 2014; Sargsyan et al., 2014; Mao et al., 2016). When these model parameters represent measurable quantities, the sensitivities can provide useful feedback about which observations are needed to better reduce variability.

Though there is a general expectation that peatland C cycling may be altered by climate change arising from warmer temperatures, elevated CO_2 concentrations, and lower water tables (e.g., Roulet et al., 1992; Moore et al., 1998; Freeman et al., 2004; Strack et al., 2004; Bridgham et al., 2008; Fenner and Freeman, 2011; Wu and Roulet, 2014), most studies draw conclusions from small-scale experimental manipulations or long-term observational studies; few studies use large-scale and long-term experimental manipulations

coupled with peatland models to evaluate changes across a range of future climate scenarios. The Spruce and Peatland Responses Under Changing Environments (SPRUCE) project is addressing an important gap in the understanding of peatland ecosystem responses to climate change (Krassovski et al., 2015; Wilson et al., 2016; Hanson et al., 2017). The overall objective of SPRUCE is to examine the responses of various ecosystem processes to a range of future temperatures under ambient and elevated CO_2 concentrations. The SPRUCE project uses 10 large (12-m diameter) enclosures to increase air and soil temperatures (+0°C, +2.25°C, +4.5°C, +6.75°C, and +9°C) under both ambient and elevated (+500 parts per million) CO_2 concentrations for 10 yr in an ombrotrophic bog in north-central Minnesota, USA. Importantly, this regression-based design (Cottingham et al., 2005) permits the evaluation and parameterization of temperature response curves, allowing for the assessment of the nonlinearity of such responses.

Modeling is an integral part of the SPRUCE project, and simulations are performed both to examine the sensitivity of model parameters and the effects of the experimental manipulations, and to predict the impacts of climate change on peatland ecosystem processes over larger spatial and temporal scales than would be achievable in the field experiment. Critical to the interpretation of peatland ecosystem responses to climate change is the thorough characterization of pretreatment conditions in the field, including quantification of both spatial and temporal variation, and a sensitivity analysis of the peatland model to identify which ecosystem parameters contribute most to model prediction uncertainty. Therefore, we took advantage of the rich pretreatment datasets collected as part of the SPRUCE project to: (i) characterize and compare temporal vs. spatial variation in peatland characteristics, with a primary focus on C cycle processes; (ii) determine the key parameters contributing variations in C fluxes in a peatland C model; and (iii) discuss the implications of variation in peatland ecosystem properties, particularly net peatland C fluxes and peat C stocks, on the analysis and interpretation of warming and CO_2 responses in the SPRUCE experiment.

The environmental and ecosystem process data described in this paper were collected to characterize the pretreatment conditions prior to the start of the SPRUCE experiment. However, because of the wealth of data collected, we were able to use these data to address the objectives of this paper; specifically, to compare spatial vs. temporal variability in several ecosystem process measurements and evaluate how this variability may affect the interpretation of treatment effects from a large-scale manipulation. In many instances, the data were not collected at multiple scales and thus the objective of this paper was not to evaluate at which spatial or temporal scale a given measurement was most variable, but rather to compare spatial and temporal variability for a given measurement. However, some parameters (i.e., fine-root biomass production, peak standing crop, and peat chemistry data) were compared at multiple spatial scales (across the bog vs. hummock–hollow), across plots, and across multiple depths. Overall, the presented data are applicable to the S1 bog and the objective was not to characterize spatiotemporal variability across black spruce bogs in general.

MATERIALS AND METHODS
Site Description

This study took place at the S1 bog, an ombrotrophic peatland located in the Marcell Experimental Forest in north-central Minnesota (Sebestyen et al., 2011a). The vegetation is primarily composed of tall-statured vegetation, mainly black spruce [*Picea mariana* (Mill.) B.S.P.] and larch [*Larix laricina* (Du Roi) K. Koch]; shrubs, primarily *Rhododendron groenlandicum* (Oeder) Kron and Judd and *Chamaedaphne calyculata* (L.) Moench; sedges [*Eriophorum vaginatum* (L.) and *Eriophorum viridicarinatum* (Engelm.) Fernald]; herbs [*Maianthemum trifolium* (L.) Sloboda]; and *Sphagnum* mosses [*Sphagnum angustifolium* (C.E.O. Jensen ex Russow) C.E.O. Jensen, *Sphagnum fallax* (Klinggr.) Klinggr., and *Sphagnum magellanicum* Brid.]. The bog has a hummock–hollow microtopography, with a typical relief of approximately 30 cm (J. Graham, personal communication, 2016).

The S1 bog has been the site of long-term hydrological and biogeochemical measurements by the USDA Forest Service and was the site of a manipulation study evaluating the effects of bog vegetation harvest on hydrology (Sebestyen and Verry, 2011; Sebestyen et al., 2011b). The bog was harvested in two strip cuts, first in 1969 and then in 1974. Within this historical context, the SPRUCE experiment occupies the location of the 1974 strip cut, as the lower tree density facilitated construction of large experimental enclosures that encompassed the treetops (Fig. 1). This site is representative of a naturally regenerated stand following aboveground tree removal from black spruce logging.

Three transects were established in the southern half of the bog, with plots connected via spur boardwalks to each main transect boardwalk (Fig. 1). An octagonal boardwalk surrounds each plot, and plot measurements were made within the 12-m diameter plot interior. A total of 17 plots with octagonal boardwalks were established. Each plot is located approximately 20 m from the next nearest plot. Ten of the 17 plots were designated as experimental plots and are the locations where the experimental enclosures were built (Hanson et al., 2017). The seven remaining plots served as ambient measurement plots. Depending on the variable, measurements were reported from four ambient plots, the 10 designated experimental plots, 12 plots (10 experimental and 2 ambient), or 16 or 17 plots (all plots, both ambient and experimental). The plots were the focus of our measurement efforts, given the design of the SPRUCE experiment, and thus represent the primary emphasis for this analysis of spatial vs. temporal variability. Measurements also occurred outside the plots and these measurements were collected either in between the plots or in the south or north ends of the S1 bog (Fig. 1). Measurements outside the plots were included in this analysis, as plot-level measurements were not yet available for certain variables. In the south end of the bog, measurements were collected within a roughly 50 by 40 m area, and in the north end of the bog, measurements were collected directly off a linear boardwalk that is approximately 80 m in length. The specific plots or locations in the S1 bog in which each measurement was collected are listed in Supplemental Table S1.
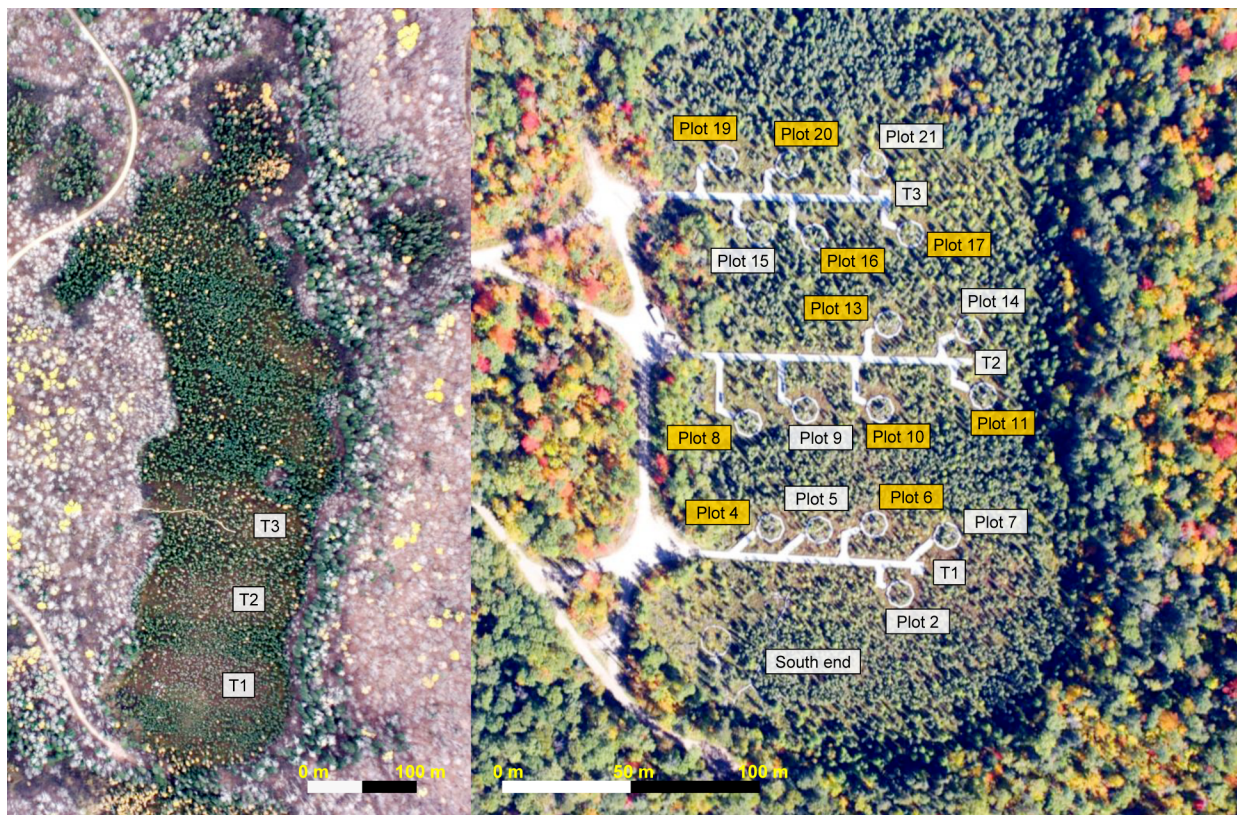
Fig. 1. Aerial photographs of the S1 bog taken in October 2011 (left) and September 2014 (right). The left image shows the entirety of the S1 bog, including the visible 1974 strip cuts where the three transects (T1–T3) and Spruce and Peatland Responses Under Changing Environments project (SPRUCE) plots were established. The right image shows the location of the 17 plots with octagonal boardwalks and the southern end of the bog where the pretreatment measurements were also collected. The 10 plots that received experimental enclosures are identified with orange shading, and the remaining seven plots are considered to be ambient plots.

Data in this paper are primarily from the pretreatment characterization period (i.e., data collected prior to the initiation of warming and elevated CO_2 treatments). The earliest pretreatment measurements began in 2010 but several other measurements were initiated in later years. In 2014, a deep peat heating experiment (heating targeted at 2-m peat depth) was initiated (Wilson et al., 2016; Hanson et al., 2017), and thus pretreatment measurements of depth-specific peat characteristics were collected only until 2013. However, pretreatment measurements for shallow peat or aboveground processes were collected throughout the deep peat heating period and until whole-ecosystem warming commenced in August 2015. Some data collected in 2016 were reported from four ambient plots that did not receive enclosures (plot nos 5, 7, 14, and 21; Supplemental Table S1).

Environmental Measurements and Vegetation Phenology

Environmental Measurements

Half-hourly mean air temperature was measured at the center of each of four plots using thermistors (Model HMP-155; Vaisala, Inc., Helsinki, Finland) in 2014 to 2016. The measurements reported here were made at duplicate locations 2 m above the surface of the peat.

Multipoint thermistor probes were used for automated mean half-hourly peat temperature measurements (W.H. Cooke & Co.

Inc, Hanover, PA). Peat temperatures were recorded at nine depths in each of four plots (only 0, −0.2, −0.5, and −2.0 m depths were reported here; 0 cm is the surface of the hollow) in 2014 to 2016. Because the bog surface undulates between hollow bottoms and hummock tops, a uniform basis for assessing the depth of belowground processes was needed. The hollow elevations were more regular than the hummock tops and thus hollows were chosen as the reference location. Peat temperature and other environmental measurements are referenced to the hollows with values below the hollows expressed as negative depths and values above the hollows and within hummocks expressed as positive depths.

The CO_2 concentration ($[CO_2]$) in air was measured every 6 min in the same four plots in 2015 to 2016. The $[CO_2]$ was measured by pulling air from the center of each plot at 2 m to a sampling manifold made up of three-way valves from which gas samples were analyzed with a LiCor LI-840 CO_2/H_2O meter (LiCor, Lincoln, NE). Temperature and $[CO_2]$ data are available online (Hanson et al., 2015, 2016a).

Peat depths were measured once in each of 17 plots using a segmented peat push probe (Model 403.1, AMS Inc., American Falls, ID). Peat depth was measured in eight locations per plot, and peat depth was recorded as the total probe length minus the length remaining above the peat surface.

Volumetric soil water content ($cm^3\ cm^{-3}$) was measured at 0 m (underneath the hummock at hollow height) and ~0.20 m

below the hummock surface at three locations (subplots) within 10 plots (10HS, Decagon Devices Inc., Pullman, WA) (Hanson et al., 2017). Sensor data were only available for 2 mo during the pretreatment period (summer 2015), and some sensors were out of range, resulting in 27 or 28 working sensors.

Phenology

Leaf-out (*Picea*, *Larix*), flowering (*Rhododendron*, *Eriophorum*), and senescence (*Larix*) were recorded daily at one location in the S1 bog on the basis of camera observations supplemented with weekly notes during spring and fall periods from 2010 to 2015.

Carbon Flux and Associated Measurements
Tree and Shrub-Layer Aboveground Net Primary Production

Annual assessments of tree basal area were conducted in 12 plots in February 2011 to 2015 by measuring bole circumference at 1.3 m height. As part of the SPRUCE project efforts, these data were combined with measured tree height in the following allometric equation (from tree harvests in the south end of the S1 bog) to generate an estimate of total standing live dry mass (g) per tree ($r^2 = 0.994$; $n = 42$):

$$Dry\,mass = \left(5.27 \times 10^5\right) \times \left(BA \times H\right), \qquad [1]$$

where BA is the tree basal area (m^2) and H is tree height (m). Data were converted to C equivalents assuming 48% C by mass, which was supported by plant tissue C analyses (Phillips et al., 2017). Individual tree mass data were summed by plot and the difference between years yielded annual tree aboveground net primary production (ANPP) (g C m^{-2} yr^{-1}) for a designated plot area of 66.3 m^2.

Shrub-layer ANPP was obtained through annual destructive harvests of shrub-layer vegetation in two 0.25 m^2 subplots (0.5 by 0.5 m) from 2012 to 2015. Two subplots were harvested in each of 17 plots per year. The collected vegetation, including multiple woody, forb, and sedge species, was divided into older vs. current-year stem and leaf tissues and all tissues were dried, weighed, and converted to g C (48%) for an assessment of combined shrub-layer ANPP (g C m^{-2} yr^{-1}) per plot. Actual C content for various species and tissues varied from 46 to 53% (Phillips et al., 2017).

Sphagnum Net Primary Production

Estimates of *Sphagnum* net primary production (NPP) required a combination of measurements and scaling assumptions. The primary measurement of *Sphagnum* growth in 2012 to 2015 in 12 plots was the increase in the length of individual *Sphagnum* stems, estimated via methods adapted from Clymo (1970). Brush wires (Rydin and Jeglum, 2013) were used in hummocks from May to October and bundles of 10 5-cm long stems (S.D. Bridgham, personal communication, 2016) were deployed in hummocks from October to May (to capture early spring growth) and in hollows throughout the year. Stem growth

was converted to dry mass with data on mass per unit of stem length (Clymo, 1970) from harvested stems of the three major *Sphagnum* species present. Dry mass increment per stem was converted to an area-based estimate using data on species-specific stem density (stems cm^{-2}), which were obtained by counting the stems in six replicate cores 8 cm in diameter. These values were expressed in C units based on laboratory analysis (Costech Analytical Technologies, Inc., Valencia, CA) of the C content of *Sphagnum* stems (43%). Finally, plot-level estimates of NPP (g C m^{-2} yr^{-1}) were determined as a weighted average of the three species based on surveys of *Sphagnum* community composition across the bog and summing the results of the May to October and October to May measurement periods.

Sphagnum and Peat NEE

Six automated clear-top chambers and the associated control system were installed in six locations (~2–20 m apart) in the S1 bog approximately 15 m from the bog margin in June 2014. *Sphagnum* carpets containing *S. magellanicum* or *S. fallax* were carefully transplanted into hollow locations at natural field density within chamber collars to test for species differences on NEE. There was no significant effect of *Sphagnum* species on NEE, so the data were combined to represent *Sphagnum* NEE in this paper. The automated clear-top LI-COR 8100–104C chambers (20 cm in diameter) (LiCor) equalize chamber pressure with atmospheric pressure and maintain a well-mixed air sample, taking near-continuous readings over 120 s using nondispersive infrared technology from each chamber every hour with a deadband of 30 s. The deadband represents the period of time when the automated chamber is closed and mixing, and these data are not included in the NEE calculation. The NEE measurements were made during conducive weather conditions (i.e., no snow cover or flooding) from June to November 2014. Daily mean values of NEE were used to calculate the mean monthly NEE.

Fine-Root Production and Peak Standing Crop

Nondestructive minirhizotron technology was used to quantify patterns in the distribution and dynamics of plant fine roots (i.e., ephemeral roots less than 2 mm in diameter, responsible for plant water and nutrient acquisition) across gradients of microtopography. Minirhizotrons are clear tubes permanently installed into the peat profile, and the upper surface of the minirhizotron is repeatedly imaged over time with a specially designed camera. Individual roots in each minirhizotron image are assessed for their length and diameter to quantify fine-root births, growth, and deaths over time (Iversen et al., 2012).

A total of 24 cellulose acetate butyrate minirhizotrons (Bartz Technology Corporation, Carpinteria, CA) were installed at a ~45° angle to a depth of ~80 cm in July 2010. The minirhizotrons were installed in 12 locations across the bog, in paired hummock–hollow microtopographies in each location ($n = 2$ minirhizotrons in each location, 24 minirhizotrons in total). Minirhizotrons were installed across gradients of tree density at the southern and northern portions of the S1 bog to capture the intrinsic diversity in plant

cover across the bog. The overstory of the bog was dominated by *P. mariana* and *L. laricina* (with *P. mariana* making up 97% of the basal area on average within a 5-m radius of the minirhizotrons), whereas the understory was dominated by ericaceous shrubs, which ranged in cover from 34 to 61% across the minirhizotron locations. Sedges and forbs averaged less than 10% cover across all locations (Iversen et al., 2017a).

Images were collected from the upper surface of the minirhizotrons weekly during the growing seasons of 2011 and 2012 (BTC-100× minirhizotron camera, Bartz Technology Corporation, Carpinteria, CA), and analyzed for the length and diameter of individual roots by the same technologist (RooTracker software, Duke University, Durham, NC). Although images were collected throughout the entirety of the peat profile from 0 to 80 cm, most roots were found in aerobic surface peat above the average water table depth (Iversen et al., 2017a). Root production was measured as an increase in root length or the birth of a new root between imaging dates, and peak standing crop was the maximum amount of fine root length observed during the growing season per minirhizotron location. Root length and diameter were converted to root biomass using species-specific allometric relationships developed for the dominant vascular plant species in the bog (Iversen et al., 2017a). Annual fine-root biomass production and peak standing crop for trees and shrubs were extrapolated to biomass per m^2 of peat by accounting for minirhizotron image size and angle of installation, and by assuming a 2-mm depth of field for each minirhizotron image (e.g., Iversen et al., 2008); biomass was converted to C units with the measured fine-root percent C (54%) averaged across species-specific root voucher specimens from the S1 bog that had been oven-dried at 70°C, ground, and analyzed for C content on an elemental analyzer (Costech Analytical Technologies, Inc., Valencia, CA). The timing of root production was calculated as the weekly proportion of maximum annual fine-root production in the top 20 cm of the hummocks, where we found the majority of fine-root biomass. Fine-root biomass production and standing crop data are available online (Iversen et al., 2017b).

Photosynthesis and Foliar Respiration

Gas exchange rates (at 25°C) were measured seasonally from 2010 to 2015 on the major shrub species and both tree species. Measurements were made on visibly healthy foliage along the three transects and on trees at the south end of the bog ($n = 6–11$ locations). Branches were cut from the mid-upper canopy (trees) or the upper canopy (shrubs), recut under water, and measured immediately with portable gas exchange systems (Li-6400, Li-Cor Inc.). Use of excised tissues allowed branches from multiple plants to be measured simultaneously with multiple gas exchange systems under standardized conditions to obtain the necessary photosynthetic parameters for modeling. Prior assessments indicated that there was no difference between excised and in situ measurements for periods up to 36 h. Although these measurements allowed for assessment of the maximal rates of photochemistry under controlled con-

ditions, other work is being done in situ to assess the diurnal patterns of gas exchange under enclosure-specific conditions. We used the approach of Gu et al. (2010) as implemented in LeafWeb (http://www.leafweb.org, accessed 9 Oct. 2017) to analyze photosynthetic × CO_2 response curves and SigmaPlot processing software (version 11, Systat Software Inc., San Jose, CA) to analyze light response curves (see Jensen et al., 2015a, 2015b). Photosynthesis and respiration data for *P. mariana* are available online (Jensen et al., 2015b).

Ecosystem-Level Flux of CO_2 and CH_4

Net CO_2 flux in the dark (i.e., ecosystem respiration) and CH_4 flux were assessed approximately monthly during the growing season from July 2013 to June 2015 (Hanson et al., 2016b). A 1.2-m diameter in situ collar was installed in an area containing shrubs and *Sphagnum* but no trees at one location in each of 10 plots. The collar was used as the base for a headspace accumulation measurement of both CO_2 and CH_4 gases with open path sensors (Model 7500 for CO_2 and H_2O; Model 7700 for CH_4, LiCor Inc., Lincoln, NE) over a 2- to 4-min period (the methodology is described in detail in Hanson et al., 2016b). Data were collected monthly during the growing season and at selected cold season periods in both late fall and early spring when surfaces were frozen to various degrees. Ecosystem-level flux data for CO_2 and CH_4 are available online (Hanson et al., 2014).

Total Organic C Concentration and Yield

Pore water was collected every two weeks in 2014 from each of 10 plots. Near-surface pore water was collected from one piezometer per plot. Each piezometer was constructed out of PVC, and was 5.1 cm in diameter with a 10-cm long screened section (0.25-mm slots), and the near-surface piezometer collected pore water at 0 to −0.1 m (below the hollow surface). An unfiltered water sample was pumped from each piezometer into a clean 250-mL high-density polyethylene bottle. Total organic C (TOC) concentration was measured via high-temperature combustion on a Shimadzu TOC-VCP (Columbia, MD), and the data are available online (Griffiths and Sebestyen, 2016a).

Yields of TOC were estimated for each plot by multiplying near-surface TOC concentration by near-surface lateral outflow, which is the pathway along which most water drains to peatland outlet streams (Verry et al., 2011). Lateral water outflow was estimated at the plot scale with a prototype subsurface corral that was constructed in the south end of the bog in fall 2011. The 134-m^2 corral was constructed by inserting 10 to 11 interconnecting vinyl sheet piles per side of an octagonal corral through the peat into the underlying mineral soil (Sebestyen and Griffiths, 2016). Water from the top 30 cm of peat inside the corral drained into a slotted vertical pipe that was connected via a subsurface horizontal pipe to a collection reservoir and with a commercially available sump pump located outside the corral. Daily water yields were calculated as the daily change in water level inside the reservoir (accounting for pumping when the reservoir was full) multiplied by the cross-sectional area of the 31-cm diameter reservoir. To calculate TOC

yield, a TOC concentration was assigned every day from the date of sample collection to the next sampling date, which was multiplied by daily outflow. The TOC concentration from the bog outlet stream (measured weekly; Griffiths and Sebestyen, 2016a, 2016b) was used from April to June when pore water TOC concentrations were not measured. Total organic C yield (g C m^{-2} yr^{-1}) was estimated for the ice-free period when water and TOC flowed from near-surface peat (April–September). Since outflow data were extrapolated from a single site to each plot, spatial variation in TOC yield reflects TOC concentration differences among plots.

Depth-Specific Peat and Pore Water Chemistry and Fine-Root Biomass Density
Peat Chemistry

Spatial variation (across the bog and by depth) in peat C, C/N ratio, C/P ratio, and bulk density were determined in the summer of 2012 from 16 plots (Iversen et al., 2014). Surface peat (0 to –0.3 m) was collected using a modified hole saw, but deeper peat (–0.3 to –2 m) was collected with a peat corer (Watermark Russian sediment borer, Forestry Suppliers, Inc., Jackson, MS). Once extracted, all cores were sectioned into 0.1-m increments to a depth of –1 m, and 0.25-m intervals from –1 to –2 m. Two to three cores per plot were collected, and samples were combined (i.e., one core per plot) for analysis of bulk density (g cm^{-3}), and total C, N, and P (g g^{-1}). Carbon and N concentrations were analyzed by combustion on a TruSpec elemental analyzer (TruSpec CN Model #630-100-100, LECO Corporation, St. Joseph, MI). Phosphorus concentration was analyzed via HNO$_3$ microwave digestion followed by inductively coupled plasma spectrography on a Thermo Jarrell-Ash model 61E inductively coupled plasma spectrograph at the University of Georgia. Peat chemistry data are available online (Iversen et al., 2014).

Peat ^{14}C and [13]C

Samples for ^{14}C and ^{13}C analysis came from the same cores collected for peat chemistry analysis and were performed to enable quantification of peat and C accumulation rates and infer changes in C cycling within the bog over the past 10,000 yr (Hobbie et al., 2016; K.J. McFarlane, unpublished data). Samples were prepared by sealed-tube combustion to CO$_2$ in the presence of CuO and Ag and were then reduced onto Fe powder in the presence of H$_2$ (Vogel et al., 1984). Radiocarbon values were measured in 2013 on the Van de Graaff FN accelerator mass spectrometer at the Center for AMS at Lawrence Livermore National Laboratory. The δ^{13}C values were determined at the Department of Geological Sciences Stable Isotope Laboratory at University of California-Davis with a GV Optima Stable Isotope Ratio Mass Spectrometer (Fisons, Manchester, UK). Radiocarbon isotopic values were corrected for mass-dependent fractionation with measured δ^{13}C values and were reported in Δ^{14}C notation corrected for ^{14}C decay since 1950 (Stuiver and Polach, 1977). Peat ^{14}C and ^{13}C data are available online (Iversen et al., 2014).

Pore water TOC

Pore water for depth-specific analysis was collected every two weeks in 2013 from one nest of piezometers in each of the 16 plots. The piezometer design and sampling methodologies were the same as described above, except that additional piezometers were sampled with screens that opened at deeper depths below the surface (–0.3, –0.5, –1.0, –2.0, and –3.0 m). Pore water TOC concentration data are available online (Griffiths and Sebestyen, 2016a).

Fine-Root Density

Root ingrowth cores were installed to capture the biomass of newly grown fine roots. Ingrowth cores were constructed from rigid polypropylene tubes (7.3 cm i.d.) with a 5-mm mesh containing a 50% open area and filled with root-free commercial peat harvested from a nearby bog. Paired hummock and hollow cores were installed to a depth of –0.3 m in six locations in the south end of the bog in June 2013 and collected in October 2013. All fine roots were carefully removed from each 0.1-m core section with forceps and were oven-dried at 70°C and weighed. Root biomass density was calculated from the total dry mass of all roots per m^3 of peat (this was subsequently converted to g C m^{-3}, assuming 54% C from the C content analysis described above).

Quantifying Variation in Empirical Measurements

We sought to quantify the variation contributing to uncertainty in estimates of environmental variables and C cycle parameters in the S1 bog. Here, we use a broad definition of uncertainty that includes spatial and temporal variation in a given process, measurement and analytical error, and model parameter uncertainty. From an empirical standpoint, we focused on measuring and comparing spatial vs. temporal variations in environmental and C cycle parameters. Additional sources of uncertainty, such as measurement or analytical error, were not analyzed in this assessment. Therefore, we use the term "variation" to describe this level of uncertainty in our measured processes in the field. From a modeling standpoint, we focus on model parameter uncertainty, which includes spatial variability in environmental characteristics and uncertainty about model processes (see the following section for details).

Spatial and temporal variation in a given measurement was calculated as SD and CV (expressed as a percentage). The CV was used to compare temporal vs. spatial variation for a given process and among processes, as CVs are a standardized value describing variation relative to the mean. However, CVs were not computed for interval-scale data (e.g., phenological observations); instead, SDs were reported. For temperature, CVs were calculated from data in degrees Kelvin but mean values were reported in Celsius for ease of interpretation.

Annual Net C Flux and Peat C Standing Stock Calculations and Propagating Variation

From the individually measured C cycle processes described above, annual net C flux and peat C standing stock, and the spatial variation in each, were calculated. Temporal variation in net

C flux was not assessed, as not all components used to calculate net C flux (e.g., TOC efflux) were measured in multiple years. Similarly, temporal variation in C standing stock was not assessed as peat sampling was only conducted in 2012.

Annual net C flux was calculated from annual estimates of aboveground NPP (trees, shrubs, and *Sphagnum*), belowground NPP (tree and shrub roots), and annual C losses via heterotrophic CO_2 efflux, net CH_4 efflux, and TOC efflux. The SD associated with each component of net peatland C flux was calculated and reflected the spatial variation (i.e., among sampling locations) in those measurements. The spatial SDs for interpolated annual heterotrophic CO_2 efflux and CH_4 efflux were derived from multiple probabilistic runs for fitted apparent temperature response curves from the pretreatment data (Hanson et al., 2016b). Nonlinear regression estimates for base respiration, Q_{10} values (i.e., the rate of change of respiration over 10°C), and their respective SD values from the fitted equations in Hanson et al. (2016b) were applied to annual runs for the climate years of 2011 to 2014. The CH_4 efflux interpolation used a similar calculation with a water table term. The SD of net C flux was propagated with the additive variation propagation shown in Eq. [2] for $x + y = z$.

$$SD_Z = \sqrt{(SD_X)^2 + (SD_Y)^2}$$ [2]

A 95% confidence interval (CI) for net C flux was also calculated from the mean and SE, and was used to determine whether the C flux was different from zero (i.e., a source or sink of C). The SE was calculated for each C flux component as SD divided by the square root of the sample size, which varied from 10 to 24 depending on the individual C cycle measurement, and the SE for net peatland C flux was calculated via additive propagation [Eq. 2]. Sample sizes for CO_2 and CH_4 efflux were assumed to be 10, as these measurements were collected from 10 plots.

Peat C standing stock (kg C m^{-2}) was calculated by multiplying mean peat C content (g C g^{-1} dry mass [DM]) by mean bulk density (g DM cm^{-3}) and then by depth interval. Total C standing stock was the summation of peat C across all depths. The SD of each measurement of C content and bulk density reflected spatial variation across plots. The SD of C standing stock at each depth was propagated with the multiplicative variation propagation shown in Eq. [3] for $x \times y = z$, and then the SD of the total C standing stock across all depths was propagated via additive variation propagation [Eq. 2].

$$SD_Z = \sqrt{\left(\frac{SD_X}{X}\right)^2 + \left(\frac{SD_Y}{Y}\right)^2}$$ [3]

Peatland Model Sensitivity Analysis

We used a SPRUCE-specific version of the Energy Exascale Earth System model (ELM_SPRUCE) to conduct a sensitivity analysis of the model output to input parameters. ELM_SPRUCE is based on the previous CLM_SPRUCE model, a version of the Community Land Model, version 4.5 (Oleson et

al., 2013) that includes the hummock–hollow microtopography, horizontal transport, and wetland hydrological dynamics (Shi et al., 2015). The ELM_SPRUCE model also includes a microbial and CH_4 submodel (Xu et al., 2015), as well as a submodel for the representation of moss physiology. Here, we investigated the effects of uncertainty in both hydrology and biogeochemistry parameters on the net C flux of the S1 bog. The model parameters were assumed to follow uniform distributions within a defined range (Table 1). A number of these parameters depended on plant functional type (PFT), and four PFTs were used in these simulations to simulate the dominant types of vegetation in the S1 bog: *L. laricina* (adapted from the generic boreal deciduous needleleaf type in the Energy Exascale Earth System Model), *P. mariana* (adapted from the generic boreal evergreen needleleaf type in the Energy Exascale Earth System Model), a generic shrub type (representing *R. groenlandicum*, *C. calyculata*, and other species), and a generic *Sphagnum* type (representing *S. angustifolium*, *S. fallax*, and *S. magellanicum*). These PFTs were assumed to cover equal areas of the model grid cell for simplicity and did not change in area dynamically. A range of measurements reflecting spatial variability was used to define the bounds for specific leaf area and leaf C/N ratio (Table 1; A.M. Jensen, unpublished data, 2016). The ranges for other parameters were based on those used in previous sensitivity studies (White et al., 2000; Sargsyan et al., 2014; Shi et al., 2015). Overall, these parametric uncertainties were intended to include spatial variability in vegetation and soil characteristics and uncertainty about model processes.

To conduct the sensitivity analysis, we first equilibrated the C stocks by using preindustrial CO_2 concentrations and N deposition and continuously cycled the pretreatment meteorology observed at the S1 bog from 2011 to 2015. Default model parameters were used in this equilibration simulation. The ELM_SPRUCE model currently lacks the mechanisms to simulate the long-term accumulation of peat and predicts soil organic matter C to be about 10 times smaller than observed. At the conclusion of the equilibration simulation, the soil organic matter C profile was therefore adjusted to match the observed depth profile of peat C. The turnover time of the slowest soil organic matter C pool and the e-folding depth for soil C turnover (the depth at which the C turnover rate is about 37% of the surface rate) (Koven et al., 2013) were then adjusted so that the soil C pools remain in long-term equilibrium, following the idea of accelerated decomposition introduced in the Community Land Model (Thornton and Rosenbloom, 2005). Following this step, a transient simulation was conducted from 1850 to 1974, at which point a full harvest (removal of aboveground biomass) was performed in the model to represent the 1974 strip cuts. This transient simulation used the nearest grid cell values from a globally gridded historical atmospheric CO_2 and N deposition dataset (Oleson et al., 2013) and continued cycling the meteorology from the 2011 to 2015 period. Finally, a Monte Carlo ensemble of 3000 model simulations from 1974 to 2020 was performed by varying the parameters randomly over the prescribed ranges. In the years 2016 to 2020, we

Table 1. Model parameters and ranges of values used in the Spruce and Peatland Responses Under Changing Environments project-specific version of the Energy Exascale Earth System model (ELM_SPRUCE sensitivity analysis.

Parameter	Description	Units	PFT†	Min.‡	Max.‡
flnr	Fraction of leaf N in Rubisco§	–	All	0.05	0.3
leafcn	Leaf C/N ratio	g^{-1} C g^{-1} N	*Picea*	64.2	79.4
leafcn	Leaf C/N ratio	g^{-1} C g^{-1} N	*Larix*	57.2	71.2
leafcn	Leaf C/N ratio	g^{-1} C g^{-1} N	Shrub	20.8	44.9
leafcn	Leaf C/N ratio	g^{-1} C g^{-1} N	Sphagnum	34.2	49.8
slatop	Specific leaf area at top of canopy	m^2 g^{-1} C	*Picea*	0.00255	0.00475
slatop	Specific leaf area at top of canopy	m^2 g^{-1} C	*Larix*	0.00854	0.01302
slatop	Specific leaf area at top of canopy	m^2 g^{-1} C	Shrub	0.00833	0.0154
slatop	Specific leaf area at top of canopy	m^2 g^{-1} C	*Sphagnum*	0.002	0.008
froot_leaf	Fine root/leaf allocation ratio	–	All	0.3	2
leaf_long	Leaf longevity	yr	*Sphagnum*	0.6	1.5
Stem_leaf	Stem/leaf allocation ratio	–	*Picea + Larix*	1	3.5
Stem_leaf	Stem/leaf allocation ratio	–	Shrub	0.05	0.5
Croot_stem	Coarse root/stem allocation ratio	–	Tree + shrub	0.05	0.8
mp	Ball–Berry slope parameter	–	Tree + shrub	5	12
crit_onset_gdd	Growing degree-days for leaf-out	degree-day	N/A	25	500
bdnr	Bulk denitrification rate	–	N/A	0.001	0.75
qflx_h2o	Surface runoff rate parameter	–	N/A	0	8.00×10^{-8}
rsub_top_max	Subsurface drainage parameter	–	N/A	1.00×10^{-5}	1.80×10^{-5}
br_mr	Base rate for maintenance respiration	g C m^{-2} s^{-1} g^{-1} N	N/A	1.00×10^{-6}	5.00×10^{-6}
q10_mr	Q_{10} for maintenance respiration	–	N/A	1.2	3.8
decomp_depth_efolding	Heterotrophic respiration depth factor	m	N/A	0.1	0.6

† Not applicable (N/A) indicates that a single value was used across all four plant functional types (PFTs). 'All' indicates that a separate value was used for each PFT (i.e., there are four PFT-specific flnr values), but the same ranges apply across all four PFTs. Other parameters and ranges are specific to individual PFTs or PFT combinations.

‡ Minimum and maximum values were used to set the parameter ranges in the sensitivity analysis.

§ Rubisco, ribulose-1,5-biphosphate carboxylase/oxygenase; Q_{10}, the rate of change of respiration over 10°C.

recycled the 2011 to 2015 meteorology with a +9°C temperature elevation to simulate the effects of the highest warming scenario in SPRUCE. The quantities of interest from the simulation are net ecosystem productivity (NEP) from 2011 to 2015, and NEP+9 from 2016 to 2020.

Traditional global sensitivity analysis approaches generally require a large number of simulations that increase exponentially as the number of parameters rises, resulting in prohibitive costs for extensive model evaluations. Here, we varied 22 unique Energy Exascale Earth System model inputs, some of which were PFT-dependent for a total of 32 varying parameters (Table 1). The parameters represent factors controlling gross primary productivity, allocation of C to plant pools, stomatal conductance, N cycling, and maintenance respiration (defined as cellular respiration by leaves, fine roots, live stems, and coarse root pools). To reduce the computational cost, we constructed a Polynomial Chaos surrogate model via a Bayesian compressive sensing approach that "learns" the best possible surrogate from our 3000 simulations. Each simulation uses a randomly chosen set of model parameters from within the given ranges with all parameters varying simultaneously. This method enables a high-dimensional sensitivity analysis with this relatively small number of model evaluations (Sargsyan et al., 2014). Such a sensitivity analysis is also referred to as "variance-based decomposition", as it attributes model output variance to contributions from individual parameters and their interactions (Sobol, 1993; Saltelli et al., 2004). We calculated the main effect sensitivity index for each parameter, which is the contribution to the variance of an output variable (NEP or NEP+9) from that parameter averaged over the variations of the other input parameters. The 3000-simulation ensemble is also used to estimate the prediction uncertainty of NEP and NEP+9.

RESULTS
Spatial vs. Temporal Variation in Peatland Environmental Variables and Vegetation Phenology

For most of the environmental variables presented here (e.g., temperature, [CO_2]), plot-to-plot variation (as CV) was smaller than the temporal variation (minute to half-hourly data) (Table 2). In contrast, soil water in hollows varied more across subplots than across months, whereas soil water in hummocks varied more across months than across subplots (Table 2), a likely consequence of different bulk density, root presence, and air gaps within the hummocks that impacted sensor soil contact and sensor response. The hummock sensors were always much drier, and more erratic and rapid in their wetting and drying responses than the more stable hollow sensors, so there was greater variation in the soil moisture measured in hummocks over the 2-mo period than across subplots. Field observations and laboratory mesocosm measurements of hummock and hollow surface moisture content dynamics provide further support that there is more variable temporal water content

Table 2. Spatial vs. temporal variation in environmental variables measured in the S1 bog.

Environmental variable	Temporal variation			Spatial variation		
	Mean	CV	Temporal scale (n)	Mean	CV	Spatial scale (n)
Air temperature (2 m), °C†	7.8	5%	Half-hourly (2014–2016) n ≈ 20,000–35,000	7.8	0.6%	Plot-to-plot n = 4
Soil temperature (0 m), °C†	4.9	3%	Half-hourly (2014–2016) n ≈ 20,000–35,000	4.9	0.1%	Plot-to-plot n = 4
Soil temperature (–0.2 m), °C†	5.3	2%	Half-hourly (2014–2016) n ≈ 20,000–35,000	5.3	0.2%	Plot-to-plot n = 4
Soil temperature (–0.5 m), °C†	5.3	2%	Half-hourly (2014–2016) n ≈ 20,000–35,000	5.3	0.1%	Plot-to-plot n = 4
Soil temperature (–2 m), °C†	5.4	0.5%	Half-hourly (2014–2016) n ≈ 20,000–35,000	5.4	0.1%	Plot-to-plot n = 4
$[CO_2]$ at 2 m, parts per million	427.4	12%	6-min (2015–2016) n ≈ 22,000–121,000	427.4	1%	Plot-to-plot n = 4
Soil water: hollow, cm^3 cm^{-3}	0.681	23%	Monthly (2015) n = 2	July: 0.857 Aug.: 0.558	July: 30% Aug.: 32%	Subplots n = 27 n = 27
Soil water: hummock, cm^3 cm^{-3}	0.190	84%	Monthly (2015) n = 2	July: 0.207 Aug.: 0.175	July: 34% Aug.: 35%	Subplots n = 28 n = 28
Peat depth, m	N/A‡	N/A	N/A	3.06	29%	Plot-to-plot n = 17

† Temperature CVs were calculated from data in degrees Kelvin, but mean temperature values are reported in Celsius for ease of interpretation.
‡ N/A, not measured at that scale.

in the hummocks than in the hollows, which is driven by different rates of rewetting and evaporation, and depth to water table.

Peat depth varied across the 17 plots, with a mean depth of 3.06 m and a CV of 29%. The plot locations were generally selected to encompass areas of similar peat depths; variation in peat depth is larger across the entire bog (Parsekian et al., 2012).

Phenological changes began with *Larix* leaf-out in early May, followed by *Rhododenderon* flowering, *Eriophorum* flowering, and *Picea* leaf-out by mid-June. *Larix* leaf-off occurred at the end of October. All of these processes were similarly variable (similar SDs) across 6 yr, with the timing of *Eriophorum* flowering varying the least across years (Table 3).

Spatial vs. Temporal Variation in C Fluxes and Associated Measurements

Sphagnum NPP was the largest component of total system NPP, with mean *Sphagnum* NPP ranging from 208 to 234 g C m^{-2} yr^{-1} (Table 4). *Sphagnum* NPP variation was similar across years and across plots (the CVs were 33 and 32%, respectively). Temporal variation primarily represents the influ-

Table 3. Temporal variation in vegetation phenology measured in the S1 bog.

Phenological observation	Temporal variation		
	Mean	SD	Temporal scale (n = 6)
Larix leaf out, DOY †	131	7	Annually (2010–2015)
Rhododendron flowering, DOY	152	6	Annually (2010–2015)
Eriophorum flowering, DOY	148	3	Annually (2010–2015)
Picea leaf out, DOY	167	6	Annually (2010–2015)
Larix leaf off, DOY	302	9	Annually (2010–2015)

† DOY = day of year.

ence of interannual variation in environmental factors, although adjustments in measurement protocols and measurement errors also contribute. Spatial variation reflects the complex microtopography of the bog and the uncertainty in species distribution. With approximately 1.5 million *Sphagnum* stems per plot, only a very small fraction can be measured, and capturing the spatial heterogeneity across the plot is problematic.

Variability in *Sphagnum* and peat NEE varied considerably throughout the growing season (Table 4), with CVs ranging from 75 to 487% across months. The relatively large NEE CVs were probably caused by seasonality in *Sphagnum*'s physiological and microbial processes in response to changing environmental conditions (e.g., Bubier et al., 2003; Lafleur et al., 2003). The spatial variability among the six chambers was substantially less, with a CV of 37%. The CVs associated with *Sphagnum* NEE were large, as they were calculated from small mean *Sphagnum* NEE values. However, when the SD of monthly *Sphagnum* NEE was compared with the SD of *Sphagnum* NEE across the six measurement locations, the same pattern of larger temporal variation emerged (data not shown). Given the enhanced temporal resolution of automated NEE measurements, the protocol is being improved by developing methods to characterize the interaction of *Sphagnum* photosynthesizing tissues with water table depth and seasonal phenology in physiological rates (Walker et al., 2017).

Tree ANPP was more variable across plots than across years (Table 4), as tree ANPP (51 g C m^{-2} yr^{-1}) had a spatial (plot-to-plot) CV of 73% and a temporal (interannual) CV of 33%. In contrast, variability in shrub ANPP (mean 104 g C m^{-2} yr^{-1}) was similar across plots vs. across years (CVs of 33 and 26%, respectively) (Table 4).

Table 4. Spatial vs. temporal variation in peatland C cycle parameters measured in the S1 bog.

Peatland C measurement	Temporal variation			Spatial variation		
	Mean	CV	Temporal scale (n)	Mean	CV	Spatial scale (n)
Tree NPP, g C m^{-2} yr^{-1}	51	33%	Annually (2011–2015) $n = 5$	51	73%	Plot-to-plot $n = 12$
Shrub NPP, g C m^{-2} yr^{-1}	104	26%	Annually (2012–2015) $n = 4$	104	33%	Plot-to-plot $n = 17$
Sphagnum NPP, g C m^{-2} yr^{-1}	234	33%	Annually (2012–2015) $n = 4$	208	32%	Plot-to-plot $n = 12$
Sphagnum and peat NEE, µmol m^{-2} d^{-1}	June: 0.06 July: 0.28 Aug.: -1.35 Sept.: -0.40 Oct.: -0.28	June: 487% July: 157% Aug.: 75% Sept.: 136% Oct.: 88%	Daily (June–Nov. 2014) $n = 30$ $n = 31$ $n = 31$ $n = 30$ $n = 31$	-0.42	37%	Outside the plots $n = 6$
Foliar respiration (shrubs), µmol m^{-2} s^{-1}	1.02	52%	Seasonally (2010–2015) $n = 3$	June: 1.51 Sept.: 0.46 Oct.: 1.08	June: 27% Sept.: 111% Oct.: 45%	Outside the plots $n = 11$ $n = 11$ $n = 10$
Foliar respiration (trees), µmol m^{-2} s^{-1}	1.19	56%	Seasonally (2010–2015) $n = 4$	June: 1.15 July: 1.55 Sept.: 0.27 Oct.: 1.79	June: 82% July: 48% Sept.: 112% Oct.: 41%	Outside the plots $n = 6$ $n = 6$ $n = 6$ $n = 8$
Photosynthesis at light saturation (shrubs), µmol m^{-2} s^{-1}	8.72	15%	Seasonally (2010–2015) $n = 3$	June: 10.20 Sept.: 7.86 Oct: 8.10	June: 19% Sept.: 34% Oct.: 49%	Outside the plots $n = 11$ $n = 11$ $n = 11$
Photosynthesis at light saturation (trees), µmol m^{-2} s^{-1}	8.83	14%	Seasonally (2010–2015) $n = 4$	June: 10.10 July: 7.11 Sept.: 8.85 Oct.: 9.27	June: 20% July: 38% Sept.: 30% Oct.: 17%	Outside the plots $n = 6$ $n = 6$ $n = 8$ $n = 8$
Heterotrophic CO$_2$ efflux, µmol m^{-2} s^{-1}	3.62	75%	~Monthly (growing season) (2013–2015) $n = 10$	3.58	15%	Plot-to-plot $n = 10$
Net CH$_4$ efflux, µmol m^{-2} s^{-1}	0.11	109%	~Monthly (growing season) (2013–2015) $n = 10$	0.11	27%	Plot-to-plot $n = 10$
Fine–root biomass production (trees)‡	0.23	SD = 0.15†	Weekly (growing season) (2011–2012) $n = 14$	29.0	83%	Outside the plots $n = 24$
Fine–root biomass production (shrubs)‡	0.19	SD = 0.12†	Weekly (growing season) (2011–2012) $n = 14$	3.4	72%	Outside the plots $n = 24$
Fine–root peak standing crop (trees), g C m^{-2}	N/A §	N/A	N/A	55.6	120%	Outside the plots $n = 24$
Fine–root peak standing crop (shrubs), g C m^{-2}	N/A	N/A	N/A	11.5	150%	Outside the plots $n = 24$
TOC yield, g C m^{-2} yr^{-1}	N/A	N/A	N/A	14.2	2%	Plot-to-plot $n = 10$

† Standard deviations are reported instead of CVs for fine-root biomass production (temporal).

‡ Proportion of annual maximum for temporal; g C m^{-2} yr^{1} for spatial.

§ N/A, not measured at that scale. NPP, net primary production, NEE, net ecosystem exchange, TOC, total organic C.

Minirhizotron-based fine-root peak standing crop varied more than fine-root production across the bog (Table 4), and variation was generally related to the surrounding tree basal area (Iversen et al., 2017a). Local variation (i.e., hummock-hollow microtopography) was as great as the variation across the bog for production and peak standing crop, highlighting the need
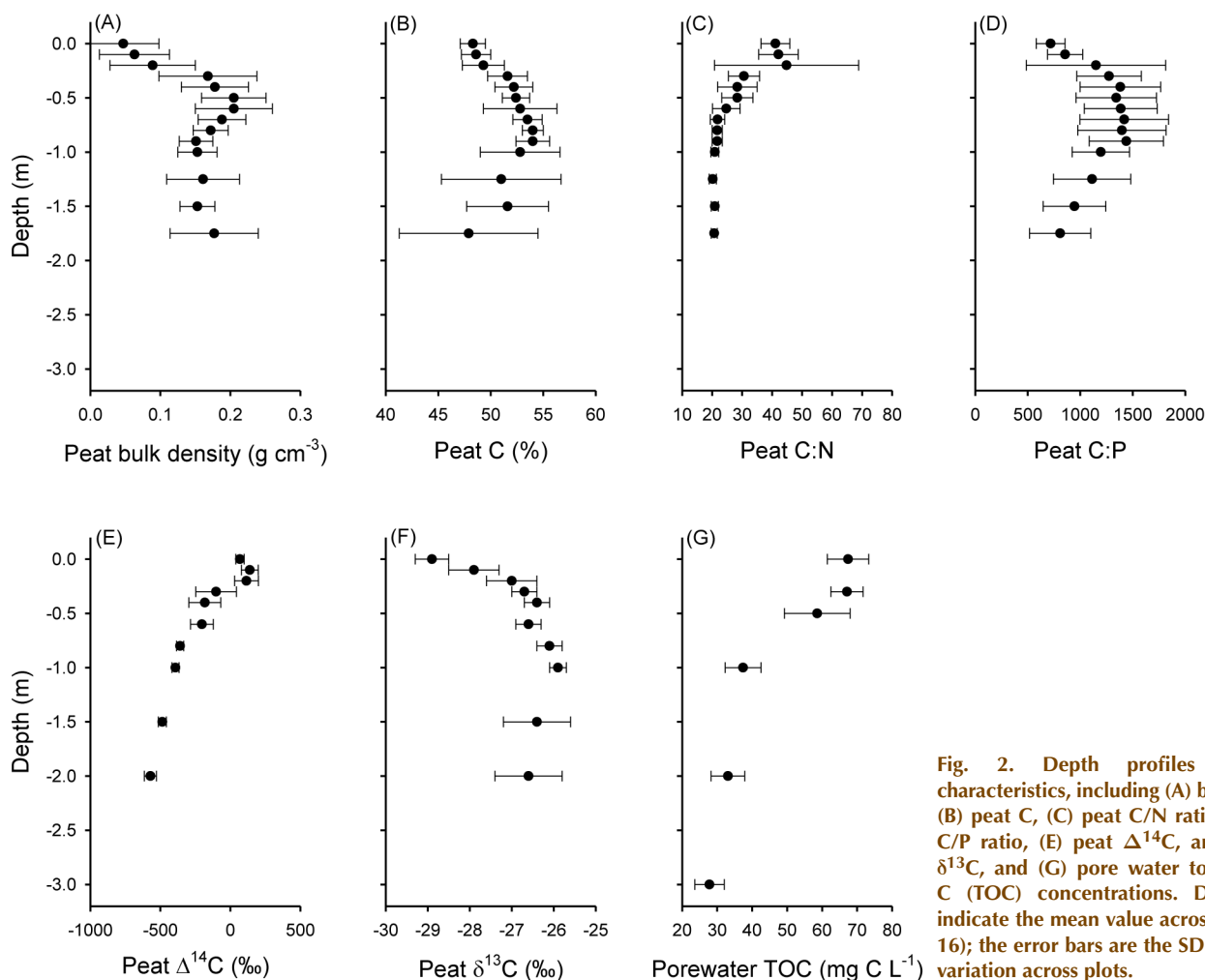
Fig. 2. Depth profiles of peat characteristics, including (A) bulk density, (B) peat C, (C) peat C/N ratio, (D) peat C/P ratio, (E) peat $\Delta^{14}C$, and (F) peat $\delta^{13}C$, and (G) pore water total organic C (TOC) concentrations. Data points indicate the mean value across plots (n = 16); the error bars are the SD and reflect variation across plots.

to capture this small-scale variation with observations. Tree fine-root biomass production was 29 g C m^{-2} yr^{-1}, with a spatial (across the bog) CV of 120% and a microtopographic (hummock vs. hollow) CV of 96%. Similar CVs were also calculated for shrub fine-root biomass production (across the bog = 141%; microtopographic = 93%). For fine-root peak standing crop, spatial (across the bog) CVs were 120% and 150% for trees and

shrubs, respectively, and microtopographic CVs were 103% and 120% for trees and shrubs, respectively.

Photosynthesis at light saturation averaged 8.83 μmol m^{-2} s^{-1} for trees and 8.72 μmol m^{-2} s^{-1} for shrubs, whereas foliar respiration averaged 1.19 μmol m^{-2} s^{-1} for trees and 1.02 μmol m^{-2} s^{-1} for shrubs (Table 4). Generally, photosynthesis at light saturation varied more across the bog than across seasons, whereas foliar respiration was similarly variable across these spatial and temporal scales. Photosynthetic rates at light saturation varied more across seasons (CVs of 52 and 56%) than did foliar respiration (CVs of 14 and 15%) (Table 4).

The heterotrophic CO_2 flux rate (3.6 μmol m^{-2} s^{-1}) was much larger than the flux of CH_4 (0.11 μmol m^{-2} s^{-1}). However, CH_4 flux varied more both across months (CV of 109%) and across plots (CV of 27%) than CO_2 flux (CVs of 72 and 15%, respectively). Overall, CO_2 and CH_4 fluxes were more variable across months than across plots (Table 4). Estimated TOC yields (reflecting variations in TOC concentration) did not vary substantially across plots and had a CV of 2% (Table 4).

Spatial Variation in Depth-Specific Peat and Fine-Root Observations

There were strong depth-specific patterns in peat chemistry, pore water chemistry, and fine-root biomass density (Fig. 2, Table 5). Generally, the peat bulk density increased with depth,

Table 5. Spatial (across the bog) and depth–specific variation in fine–root biomass density (g C m^{-3}) in hummocks and hollows. Negative depths are below and positive depths are above the hollow surface. Each depth represents a 0.1 m interval (e.g., the –0.2 m depth includes roots between –0.2 and –0.3 m).

Location and depth	Spatial variation in fine-root density†	
	Mean	CV
	————g C m^{-3}————	
Hummocks		
0.2 m	144.1	125%
0.1 m	71.2	78%
0.0 m	48.9	85%
-0.1 m	11.4	94%
Hollows		
-0.1 m	189.3	82%
-0.2 m	12.0	103%
-0.3 m	2.6	114%

† The spatial scale was outside the plots (n = 6).

the peat C and peat C/P ratio increased until −1 m and then decreased, and peat C/N ratio decreased from the surface until −0.7 m, and then was fairly stable at deeper depths (Fig. 2A–D). Peat ^{14}C was more depleted with depth, reflecting increasing peat age (K.J. McFarlane, unpublished data), whereas ^{13}C was less depleted with depth (Fig. 2E,F). Pore water TOC concentrations were higher in near surface peats than at deeper depths (Fig. 2G), possibly because of mineralization of TOC along the vertical flow path (Griffiths and Sebestyen, 2016b).

Generally, most characteristics of surface peat varied more across plots than those of deeper peat (Fig. 3). Bulk density was more variable across plots in surface peats (CV of 109%) and declined to more stable CV values across plots in deep peat (CV of 36% at −1.75 m) (Fig. 3). Peat C content was relatively invariant across plots, with slightly less variation in surface peats dominated by *Sphagnum* tissue (CV of 2%) than ancient deep peat (CV of 14%) (Fig. 3). Spatial variability in the peat C/P ratio also was greater in surface than in deeper peat, while the opposite pattern was observed for C/N ratio (Fig. 3). Plot-to-plot variability in ^{14}C was high near the peat surface with the largest variability at the −0.3 to −0.4 m depth and lower variability across plots below −0.7 m (Fig. 3). The greatest across-plot variability in ^{13}C was at the −0.1 to −0.2 and −0.2 to −0.3 m depths. Plot-to-plot variation in pore water TOC concentrations was slightly greater at deeper depths (CVs ranged from 14 to 16% at −0.5 to −3 m depths) than shallower depths (CV at 0 m was 9%, CV at −0.3 m was 7%; data not shown).

Newly grown fine-root biomass density estimated from ingrowth cores was also highly variable both laterally across the bog and vertically. In hollows, fine-root biomass density was more variable across the bog at deeper (−0.3 m) than at shallower depths (−0.1 to −0.2 m) (Table 5). In contrast, fine-root biomass
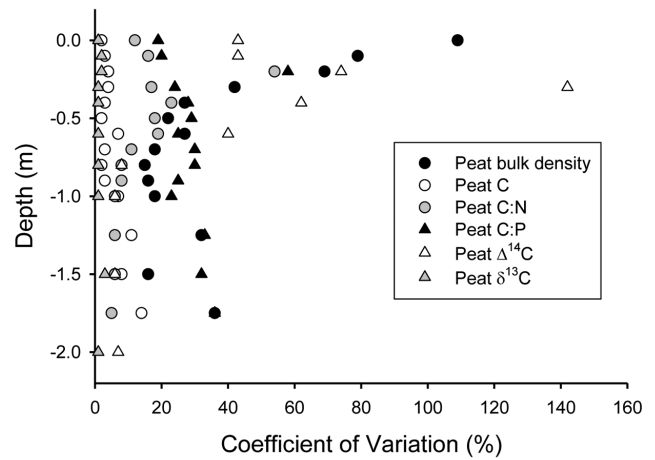

Fig. 3. Coefficients of variation (%) for depth-specific peat characteristics (peat bulk density, C, C/N ratio, C/P ratio, Δ^{14}C, and δ^{13}C). The CVs reflect spatial variation in the measured parameter at a given depth across plots, with higher CVs indicative of greater plot-to-plot variability.

density in hummocks was most variable across the bog at the shallowest depth (0.2 m) (Table 5).

Sensitivity of Net Ecosystem Production in the ELM_SPRUCE Peatland Model

Net ecosystem productivity in ELM_SPRUCE in the pre-treatment period was sensitive to 11 of the 32 model parameters investigated here (Fig. 4). Parameters were identified as being insensitive (main effect sensitivity < 0.01), as having minor sensitivity (main effect sensitivity between 0.01 and 0.05), or as sensitive (main effect sensitivity > 0.05). Parameters specific to the *Picea* PFT were the most sensitive of the four PFTs, given the ELM_SPRUCE model structure. The fraction of leaf N in ribulose-1,5-biphosphate carboxylase/oxygenase (flnr), the stem/leaf
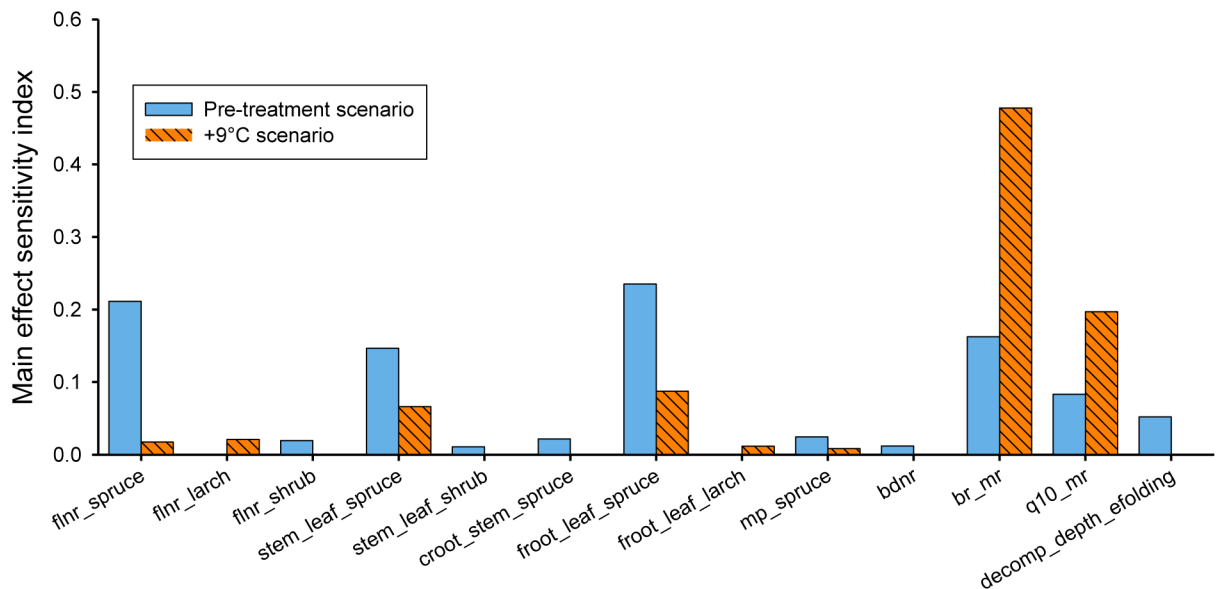

Fig. 4. Main effect sensitivity indices for the Spruce and Peatland Responses Under Changing Environments project-specific version of the Energy Exascale Earth System model (ELM_SPRUCE) parameters in the pretreatment (blue) and +9°C warming (orange) scenarios for net ecosystem productivity (NEP). Main effect sensitivities indicate the proportion of NEP variance attributed to each parameter. See Table 1 for parameter definitions.

allocation ratio, and the fine root/leaf allocation ratio were the three most sensitive PFT-specific parameters, all for *Picea*. Stem/leaf ratio and flnr had minor main effect sensitivities for shrubs, and the Ball–Berry stomatal conductance slope parameter had a minor main effect sensitivity for *Picea*. The flnr parameter was the most sensitive parameter controlling gross primary productivity (data not shown), a major component of NEP. Gross primary productivity was also a function of leaf N, which was itself a function of specific leaf area and leaf C/N. Because these two parameters were relatively well constrained by observations, only flnr was identified as sensitive. The bulk denitrification rate, the base rate for maintenance respiration, the temperature sensitivity for maintenance respiration, and the e-folding depth for decomposition, which are not PFT-specific, were also sensitive parameters. The two maintenance respiration parameters displayed the largest sensitivities. These results indicate that spatial variation in *Picea* and shrub photosynthesis and allocation characteristics, as well as maintenance respiration across all PFTs, may contribute to large variations in the pretreatment net C balance across the S1 bog.

We also analyzed the sensitivity of 5-yr average NEP to a +9°C warming scenario. In that analysis, only 8 of the 32 parameters showed significant sensitivities (Fig. 4). The relative importance of the flnr and allocation parameters declined sharply, with the exception of flnr and fine root/leaf allocation ratio for *Larix* slightly increasing in sensitivity. This may indicate the increased sensitivity of *Larix* to warming compared to the other PFTs. The growing degree-day parameter controlling spring deciduous phenology showed little sensitivity, despite a significantly lengthened growing season. The largest change in sensitivity from the pretreatment analysis was the large increase in the sensitivity of maintenance respiration parameters (base rate for maintenance respiration and temperature sensitivity for maintenance respiration). Uncertainties about the magnitude and temperature response of this respiration flux contribute strongly to uncertainty in net C fluxes in the +9°C warming scenario.

DISCUSSION
Implications of Spatial Variation on the Net C Flux Estimate for the S1 Bog

All measured C cycle parameters varied spatially in the S1 bog (Table 4), highlighting the importance of taking spatial variability into account when estimating net C fluxes. We examined how spatially explicit measures of C production from tree and shrub above- and belowground NPP and *Sphagnum* NPP, and C losses via heterotrophic CO_2 efflux, net CH_4 efflux, and TOC efflux influenced the estimate of contemporary net C flux from the S1 bog ecosystem. Overall, the mean net C flux was 8 g C m^{-2} yr^{-1} (C sink), the propagated SD was ± 105 g C m^{-2} yr^{-1}, and the 95% CI ranged from a source of 50 g C m^{-2} yr^{-1} to a sink of 67 g C m^{-2} yr^{-1} (Fig. 5). The SD reflects the large variation in C flux estimated at multiple locations across the bog. Further, the 95% CI overlapped 0 g C m^{-2} yr^{-1}, suggesting that we cannot conclude whether the bog was a net sink or a source of C despite using higher resolution process measurements that were made more frequently over space and time than what was done in many other studies. Although some of this high spatial variability could have been caused by the measurement of individual C cycle parameters at a differing number of locations in the S1 bog (n = 10–24), we used a power analysis that determined that over 600 measurements across the bog per C cycle parameter are needed for the 95% CI to be significantly different from 0 g C m^{-2} yr^{-1}. Therefore, the differing number of measurement sites probably did not solely explain the large spatial variability in the estimate of net C flux. Increasing the sample size to over 600 measurement locations is generally not realistic, especially in the context of large-scale ecosystem experiments such as SPRUCE, where the number and cost of experimental plots often limits sample size. Instead, we recognize that we cannot determine if the S1 bog is a C sink or source from pretreatment measurements because of the large spatial variability, and that this spatial variability (as 95% CI) must be taken into account when interpreting whether changes in net C flux with warming and elevated CO_2 are significant.

Of the C fluxes used to calculate net C flux, tree ANPP, and tree and shrub fine-root production were the most variable across the bog, whereas heterotrophic CO_2 efflux, net CH_4 efflux, and TOC efflux were less variable (based on their CVs). However, because *Sphagnum* NPP and CO_2 efflux were the largest C fluxes by magnitude, spatial variation in these parameters contributed most to the 95% CI.
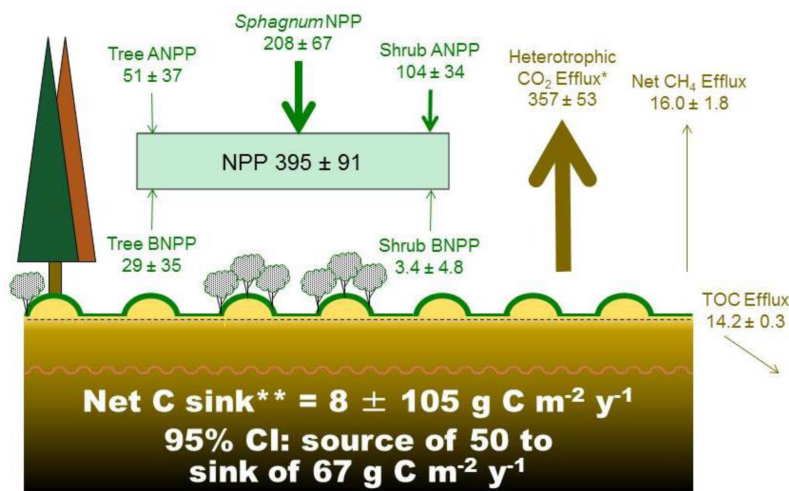
Fig. 5. The estimated mean net C flux, SD, and 95% confidence interval (CI) for the S1 bog. Net C flux was calculated as the difference in measures of above- and belowground net primary production (ANPP and BNPP, respectively), and C losses via heterotrophic CO_2 efflux, net CH_4 efflux, and total organic C (TOC) efflux (all units are g C m^{-2} yr^{-1}). Carbon flux values reflect the mean fluxes across plots or measurement locations; SDs reflect spatial variability across plots or measurement locations. Arrow widths roughly approximate the magnitude of each C flux. The SD for net C flux is the propagated variation using the SD from each C flux component. Note that additional C losses, such as isoprene and terpene emissions, dissolved inorganic C (DIC) and dissolved gas (CO_2, CH_4) export in stream flow, and CO_2 and CH_4 emissions from the peatland outlet stream were not included.

The drivers of spatial variation vary among C cycle measures. Variation in tree NPP across the plots probably reflects spatial variation in tree density and composition (*Picea* vs. *Larix*). Variation in fine-root production probably reflects the complex patterning in vegetation distribution and microtopography across the bog as fine-root production was just as variable between adjacent hummocks and hollows as it was across the bog (Iversen et al., 2017a). Variation in belowground NPP may also be large because fine-root production is notoriously difficult to quantify (Iversen et al., 2017a). Spatial variation in *Sphagnum* NPP may reflect microtopographic variations and variability in *Sphagnum* species distribution. Spatial variability in *Sphagnum* stem density, which was not surveyed, would also affect the accuracy of our estimates. The variability in TOC yields was very low compared with the other C flux components, and the low CV solely reflected variation in near-surface pore water TOC concentrations across plots, as plot-specific data on near-surface lateral outflow were not available for the pretreatment period. It is expected that spatial variation in TOC yields would have been larger if among-plot variability in both TOC concentration and lateral water outflow were quantified (e.g., Roulet et al., 2007; Nilsson et al., 2008). Spatial variations in tree physiology and root production are also a result of a small physical sample size: the gas exchange cuvette was just 6 cm^2 for physiological measurements and the summation of root observation windows across a minirhizotron surface was only ~250 cm^2 (most of which is root-free); however, there are multiple m^2 of leaf area and root area so that observations reflect just 0.01or 0.001 of a percent of the actual area. In contrast, larger integrated measurements such as the large CO_2 and CH_4 flux collars encompass almost 4% of the plot surface area; however, there was still considerable spatial variation in these measurements.

At least four studies have evaluated contemporary net C fluxes from peatlands, including measurements of NEE, and CH_4 and DOC flux, over multiple years. All four peatlands were C sinks (Table 6; Roulet et al., 2007; Nilsson et al., 2008; Dinsmore et al., 2010; Koehler et al., 2011); however, there was considerable interannual variation in C flux. This high interannual variation in the Atlantic blanket bog and Mer Bleue bog (reflecting the large SDs; Table 6) suggested that the determination of whether these peatlands were C sinks or C sources varied year to year. Similarly, we could not determine if the S1 bog was a net sink or source of C on the basis of the 95% CI estimate, which reflected high spatial variability in our multiple measurements of C cycle parameters across the bog. Reduction in measurement variability and improved empirical and projected estimates of net C fluxes in the future will require a full understanding of the contribution of each component of the flux, reducing measurement error by refining measurement techniques, and increasing sampling density.

Model Assessment

The ensemble of simulations by ELM_SPRUCE predicted the S1 bog to be a C sink for nearly all parameter combinations, which is somewhat inconsistent with the empirical assessment (Fig. 6). Specifically, when CH_4 and TOC effluxes were not included in the empirical estimate for a more direct comparison with the model output, the same conclusion was reached in that we could not determine if the S1 bog was a net sink or source of C on the basis of the 95% CI estimate (Fig. 6). In the simulations, the net C sink was primarily driven by tree regrowth following the 1974 strip cut, with some contribution from CO_2 fertilization and N deposition. However, the model experiment used only 5 yr of pretreatment meteorology, which was cycled for the entire simulation. Those years (2011–2015) may be significantly different from the longer-term record because of multiyear oscillations or trends in temperature and precipitation caused by climate change (Sebestyen et al., 2011a). If this is the case, the ELM_SPRUCE input drivers must be extended

Table 6. Comparison of net C fluxes for peatlands across the globe. In all studies, net ecosystem exchange (NEE) and net ecosystem production (NEP) are measurements or estimates of net C uptake; CH_4 and dissolved organic C (DOC) (or total organic C, TOC) fluxes are C losses.

Peatland	Net C flux† (mean ± SD)	NEE or NEP (mean ± SD)	CH_4 efflux (mean ± SD)	D/TOC efflux (mean ± SD)	Scale (n)	Citation
	—————————g C m^{-2} yr^{-1}—————————					
Atlantic blanket bog, southwest Ireland	29.7 ± 30.6	47.8 ± 30.0	4.1 ± 0.5	14.0 ± 1.6	Temporal (n = 6 yr)	Koehler et al., 2011
Auchencorth Moss, Scotland‡	89.0 ± 39.7	114.8 ± 30.1	0.3 ± 0.04	25.4 ± 9.6	Temporal (n = 2 yr)	Dinsmore et al., 2010#
Degerö Stormyr mire complex, northern Sweden§	27.0 ± 7.0	51.5 ± 4.9	11.5 ± 4.9	13.0 ± 1.5	Temporal (n = 2 yr)	Nilsson et al., 2008#
Mer Bleue bog, Ontario, Canada	21.5 ± 39.0	40.2 ± 40.5	3.7 ± 0.5	14.9 ± 3.1	Temporal (n = 6 yr)	Roulet et al., 2007
S1 bog, Minnesota	8.2 ± 105.1	38.4 ± 105.1¶	16 ± 1.8	14.2 ± 0.3	Spatial (n = 10–24 locations)	This study

† Net C flux is calculated as: NEE or NEP – CH_4 efflux – DOC (or TOC) efflux.

‡ Additional C fluxes were measured in this study, including DOC inputs, CO_2 and CH_4 loss via stream evasion, and CO_2, CH_4, particulate organic carbon, and dissolved inorganic carbon lost via stream export.

§ Additional C fluxes were measured in this study, including TOC inputs, and CO_2 and CH_4 lost via stream export.

¶ Reported as net primary production (NPP) minus heterotrophic CO_2 efflux.

Additional C flux components reported in Nilsson et al. (2008) and Dinsmore et al. (2010) (see notes above) were not included in the estimate of C balance to directly compare C fluxes across studies.

to include a longer climate record for a more accurate hindcast. Furthermore, we did not explore the sensitivity of CH_4 fluxes to parameters for the CH_4 submodel, or the export of TOC in stream flow; these CH_4 and TOC sensitivities will be explored in future ELM_SPRUCE sensitivity analyses.

In the ELM_SPRUCE model ensemble, there was a significant shift toward a smaller C sink or a minor C source during the first 5 yr under the most extreme experimental warming scenario (Fig. 6). Gross primary productivity increased because of a higher N mineralization rate and a longer growing season, but autotrophic and heterotrophic respiration increased to a greater degree for most of the model ensemble members (data not shown). The distribution of outcomes was also broader, with a longer tail on the C source side (Fig. 6), indicating the possibility of the S1 bog (or areas within the bog with specific properties) shifting toward a significant source of C. In general, parameter uncertainty and variability contributed to higher uncertainties in NEP under the warming scenario than under pretreatment conditions. The sensitivity analysis also indicated the shifting importance of specific processes (Fig. 4), providing potentially useful guidance about which ecosystem properties should be better constrained by measurements. For example, measuring spatial variation in plant respiration at different temperatures should be a high priority given these results. The sensitive allocation parameters should be constrained with recurring measurements of stem, leaf, and root growth; flnr and the Ball–Berry stomatal conductance slope parameter can be constrained with leaf-level chamber measurements.

Implications of Spatial Variation on Peat C Stock Estimates for the S1 Bog

Another important measure of peatland C is an estimate of peat C standing stock. This C cycle measure is typically calcu-
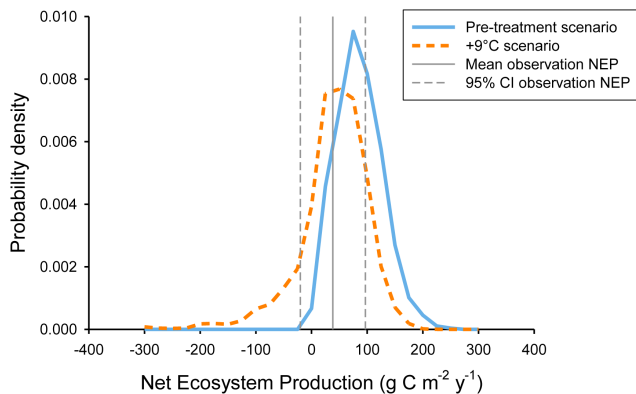

Fig. 6. Distribution of pretreatment (blue) and the +9°C warming scenario (orange) 5-yr average net ecosystem production (NEP) from the 3000 Spruce and Peatland Responses Under Changing Environments project-specific version of the Energy Exascale Earth System model (ELM_SPRUCE) ensemble members. The empirical assessment of the mean NEP for the S1 bog (solid vertical gray line; net C sink of 38 g C m^{-2} yr^{-1}) and the 95% confidence interval (dotted vertical gray lines; C source of 20 to a C sink of 97 g C m^{-2} yr^{-1}) are shown for comparison. The empirical NEP estimate does not include CH_4 and TOC effluxes in the calculation for a more direct comparison to the model output (which also does not include CH_4 and TOC effluxes).

lated from bulk density, C content, and peat depth from a single core in a peatland, with only a few studies evaluating the variability in peatland C stocks or C accumulation rates from multiple cores (Korhola et al., 1996; Ohlson and Økland, 1998; Roulet et al., 2007; van Bellen et al., 2011; K.J McFarlane, unpublished data). We estimated mean C standing stock in 2 m of peat in the S1 bog from multiple spatially explicit measurements of bulk density, peat C, and peat depth and calculated the variation (as SD) from these multiple measurements. The S1 bog peat C standing stock was 158 ± 14 kg C m^{-2} (CV = 9%). Plot-to-plot variability in peat C standing stock was greater in surface than in deeper peats (Fig. 7), following the pattern for peat bulk density (Fig. 3); the CVs mainly reflected the variation in peat bulk density rather than peat C (Fig. 7B). However, peat chemistry samples were only measured on a 2-m core, yet mean peat depth (determined from the push probe data) was 3.06 ± 0.87 m (Table 2). If the bulk density and C content data from the deepest core section (−1.75 to −2 m depth) were applied to the −2 to −3.06 m depth interval, the estimate of peat C standing stock would increase to 248 ± 37 kg C m^{-2} (CV = 15%). Further, if one SD was added (3.93 m) or subtracted (2.19 m) from the mean peat depth, then the standing stock estimate varied from 322 ± 64 (CV = 20%) to 175 ± 16 kg C m^{-2} (CV = 9%). The wide range in mean peat C stock estimated with different assumptions of mean peat depth are large, especially relative to the calculated SDs, and suggests that an accurate measure of peat depth is most important when upscaling peat C stocks to an entire peatland. The S1 bog peat C stock calculated to 2 m (158 kg C m^{-2}) was very similar to the midpoint organic C content for the upper 2 m of histosols in the United States (140 kg C m^{-2}), whereas the range in C stock estimated for the S1 bog (175–322 kg C m^{-2}) was only slightly smaller than the range in C content of histosols across the United States (64–244 kg C m^{-2}) (Guo et al., 2006).

Additional Sources of Uncertainty

Although our study focused on describing and comparing spatial vs. temporal variation in peatland ecosystem processes, we recognize that sources of error not analyzed here may contribute to uncertainty in a given variable (e.g., Yanai et al., 2012). For example, studies measuring contemporary net C fluxes via eddy covariance typically assume a random error of 20% for 30-min NEE estimates, with propagation of those errors being used to calculate the error in daily and annual NEE (Roulet et al., 2007; Nilsson et al., 2008). Analytical errors in the measurement of TOC, dissolved inorganic C, and CH_4 concentrations in stream water can also contribute to uncertainty in estimates of C flux. Nilsson et al. (2008) attributed SDs of 5 to 10% for TOC, dissolved inorganic C, and CH_4 fluxes as a result of analytical uncertainty and errors in the measurement of stream flow (from errors in stage-discharge calibrations and logger failures), whereas Roulet et al. (2007) attributed a SD of 40% to DOC fluxes on the basis of similar measurement errors. Similar sources of error can be attributed to estimates of peatland C standing stocks, including errors in

analytical measurements of peat C content and bulk density, and investigator error in the measurement of peat depths.

Concluding Remarks: Implications of Spatial and Temporal Variability for Interpreting Results from the SPRUCE Experiment

In our pretreatment characterization of the S1 bog in preparation for a large-scale climate change experiment, we found that there was significant variation in many environmental and ecosystem process variables. Environmental variables, such as air and soil temperature and [CO_2], which were measured at high temporal frequencies (i.e., 6–30 min), were more variable over time than across plots. Large temporal variation was expected because of the high frequency at which data were collected and the diurnal patterns and seasonality generally observed for such processes. Minimal spatial variation suggests that the environmental conditions reported in Table 2 were generally similar across plots. Because the plot is the experimental unit in SPRUCE, it is probably not necessary to account for these small differences in environmental conditions among plots when interpreting treatment responses in SPRUCE (e.g., using a blocked statistical design).

Aboveground vegetation phenology also varied little across the 6-yr measurement period. Increasing temperatures are expected to change the timing of vegetation phenology, including leaf-on and leaf-off dates (Ahas et al., 2002; Norby et al., 2003; Badeck et al., 2004), and these changes will logically cascade to affect C fluxes (Piao et al., 2007; Richardson et al., 2013). Because of the low interannual variation in aboveground vegetation phenology over a 6-yr pretreatment period, we expect that changes in the timing of phenological events caused by warming will be detectable if the shifts are on the scale of several days. For example, on the basis of the 95% CIs, the timing of phenological events may be significantly different from those of the pretreatment if they occur more than 3 d (*Eriophorum* flowering; 95% CI = 145–151 day of the year) to 9 d (*Larix* leaf off; 95% CI = 293–311 day of the year) earlier or later than the mean day of the year for the given phenological event (Table 3).

Many C cycle processes were also quite temporally variable, including interannual variation in ANPP and monthly variation in heterotrophic CO_2 efflux and net CH_4 efflux. Interannual variability can, in part, reflect variation in climate conditions, with many studies in peatlands pointing to the change in the water table level across years driving C fluxes (Shurpali et al., 1995; Waddington and Roulet, 1996, 2000; Roulet et al., 2007). It is likely that over the 10-yr SPRUCE experiment, C cycle processes will vary across years in response to variations in climate (e.g., dry vs. wet years). Because the experimental treatments are imposed over ambient conditions in SPRUCE (e.g., +0 to +9°C above ambient temperatures), the background interannual variability in environmental conditions (e.g., temperature, precipitation) should be consistent across treatments. However, enclosure artifacts will have to be considered when interpreting treatment effects (see Hanson et al., 2017).
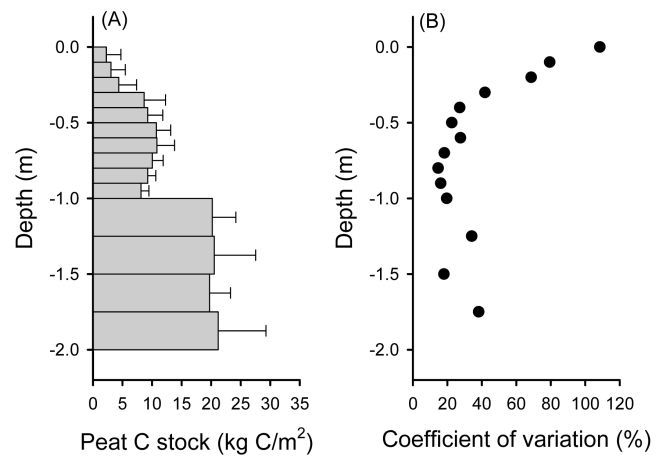

Fig. 7. Spatial variation [vertical and lateral (across the bog)] in peat C stock. (A) Mean, SD, and (B) CVs are presented at each depth. The SD associated with each depth-specific peat C standing stock value reflects multiplicative propagated variation from the SDs of peat C and bulk density at each depth. Wider bars are shown for the deepest four depth increments in (A) because the sampling increments were larger (0.25-m increments) for the -1 to -2 m depths than the 0 to -1 m depths (0.1-m increments). Peat C stock at each depth was first calculated per m^3 from the bulk density and C content data, and then expressed per m^2 after multiplying by the depth increment. The CVs reflect spatial variation in the peat C standing stock at a given depth across plots, with higher CVs indicative of greater plot-to-plot variability.

Although environmental variables (i.e., soil and air temperature, and [CO_2]) did not vary greatly across plots, several ecosystem processes varied both across plots and across the bog (e.g., tree ANPP, and root NPP), as well as by depth (e.g., peat chemistry and fine-root biomass density). For example, several peat chemical properties were more variable in surface rather than deeper peats, with the greater variability in surface peats possibly reflecting the dynamic, transiently saturated conditions of the acrotelm vs. the permanently conditions of the saturated catotelm or a change in microtopographical gradients.

It is important to note that the different processes reported here were measured at different temporal (e.g., minute to annual) and spatial (e.g., subplot to across the bog) scales. The measurement scales were selected by researchers to be the most feasible and environmentally relevant for the process of interest. It is possible that if other scales were compared (e.g., a comparison of interannual variation in temperature to plot-to-plot variation instead of half-hourly variation in temperature to plot-to-plot variation) then different conclusions of whether a process varied more spatially or temporally may be reached; however, comparing a given process measured at multiple spatial and temporal scales was not an objective of our study.

Spatial variability in pretreatment ecosystem process measurements can be difficult to account for in an ecosystem-scale experiment. The experimental design of SPRUCE is regression-based (i.e., five temperature treatments at ambient CO_2, repeated at elevated CO_2), and treatments were assigned randomly to plots within the 1974 strip cut sections that had comparable vegetation composition, peat depths, and peat chemistry. An important aspect of the regression-based design is the assump-

tion that the pretreatment measurements are not significantly correlated with the temperature differential (or daily to annual air or soil temperatures after treatment). These correlations were performed for many of the peatland measurements as part of individual investigators' assessments of spatial variation in the pretreatment data (data not shown). Even if there is no relationship between a pretreatment variable and the assigned temperature differentials, spatial variation in ecosystem processes determined during the pretreatment period should be taken into account when analyzing post-treatment effects. Multiple statistical approaches can be used, including examining the relative deviation in a given measurement between the pretreatment and post-treatment period (e.g., the analysis of TOC concentrations in Wilson et al., 2016), using before–after, control–impact (Stewart-Oaten et al., 1986), and related analyses (Underwood, 1994), randomized intervention analysis (Carpenter et al., 1989) or various time series analysis approaches (e.g., Cazelles et al., 2008; Box et al., 2016).

Spatial and temporal variation in ecosystem processes can be more thoroughly characterized if more measurements are collected, especially if those measurements encompass environmental gradients that may be driving the spatial and temporal variation (e.g., hummock vs. hollow microtopographies, wet vs. dry years). Although several years of pretreatment data are available for some of the measurements in SPRUCE (e.g., aboveground NPP and phenology, photosynthesis and respiration, CO_2 and CH_4 fluxes), pretreatment data are limited for other processes because of equipment limitations or accessibility to plots during boardwalk and enclosure construction periods (e.g., TOC efflux). Ideally, having multiple years of pretreatment characterizations across the multiple experimental plots allows for a more robust understanding of the peatland ecosystem prior to a large experimental manipulation. Increasing the number of samples across spatial scales may also reduce SE and the reported 95% CIs for a given measurement; however, there are often constraints on sampling designs. For example, the large variation in C flux estimates across measurement locations resulted in our inability to determine if the bog was a C sink or source. Instead, it was determined that >600 measurements across the S1 bog were needed to reduce variation in the 95% CI such that the CI no longer overlapped 0 g C m^{-2} yr^{-1}. Increasing the sampling size to this magnitude is not achievable, especially in an ecosystem experiment with a limited number of sampling plots (i.e., 10 experimental plots in SPRUCE). Further, each of the 10 experimental plots is 12 m in diameter, and though they are large in comparison with many other warming studies, the dedicated locations for the many environmental and ecosystem processes being measured within each plot (Table 2–Table 5) constrain our ability to collect multiple samples for a given process. Where spatial variation in an ecosystem process was identified (e.g., differences in root production in hummocks vs. hollows), efforts were made to collect data in multiple locations per plot (e.g., minirhizotrons and ingrowth cores were installed in both hummocks and hollows in each plot). During collection of pretreat-

ment and post-treatment data in an ecosystem-scale experiment, limitations such as the available measurement space and sampling and analytical costs must be weighed against accounting for variation in a given measurement via high-frequency, spatially resolved sampling.

A key goal of the SPRUCE project is the synthesis of models and observations with the goal of improving the predictability of peatland ecosystems and their feedback to the climate system. Observations of this ecosystem provide critical information for model simulations, and model predictions and sensitivity analyses are providing input into the design of observation systems within the experiment. Specifically, understanding the spatial and temporal patterns of variation within the ecosystem is important for providing inputs to model simulations and for explaining discrepancies between the model predictions and observations. As the experiment progresses, we expect the pretreatment variability described here to impact the response patterns of C fluxes and stocks to temperature and CO_2 manipulations. Interpreting these responses will probably require a further examination of pretreatment variability, understanding the new sources of variability introduced by the experimental manipulation (Hanson et al., 2017), and continuing to investigate the drivers of this variability through model sensitivity analyses as the model is further developed.

SUPPLEMENTARY MATERIAL
Supplemental Table S1. List of environmental and ecosystem process measurements collected in the S1 bog, the methodology used to collect these measurements, and the temporal and spatial scale at which the data were collected and presented.

REFERENCES
Ahas, R., A. Aasa, A. Menzel, V.G. Fedotova, and H. Scheifinger. 2002. Changes in European spring phenology. Int. J. Climatol. 22:1727–1738. doi:10.1002/joc.818

Badeck, F.-W., A. Bondeau, K. Böttcher, D. Doktor, W. Lucht, J. Schaber, et al. 2004. Responses of spring phenology to climate change. New Phytol. 162:295–309. doi:10.1111/j.1469-8137.2004.01059.x

Box, G.E.P., G.M. Jenkins, G.C. Reinsel, and G.M. Ljung. 2016. Time series analysis: Forecasting and control. 5th ed. John Wiley & Sons, Hoboken, NJ.

Bridgham, S.D., J. Pastor, B. Dewey, J.F. Weltzin, and K. Updegraff. 2008. Rapid carbon response of peatlands to climate change. Ecology 89:3041–3048. doi:10.1890/08-0279.1

Bubier, J.L., G. Bhatia, T.R. Moore, N.T. Roulet, and P.M. Lafleur. 2003. Spatial

and temporal variability in growing-season net ecosystem carbon dioxide exchange at a large peatland in Ontario, Canada. Ecosystems 6:353–367.

Bubier, J., A. Costello, T.R. Moore, N.T. Roulet, and K. Savage. 1993. Microtopography and methane flux in boreal peatlands, northern Ontario, Canada. Can. J. Bot. 71:1056–1063. doi:10.1139/b93-122

Bubier, J.L., P.M. Crill, T.R. Moore, K. Savage, and R.K. Varner. 1998. Seasonal patterns and controls on net ecosystem CO_2 exchange in a boreal peatland complex. Global Biogeochem Cycles. 12:703–714. doi:10.1029/98GB02426

Bubier, J., T. Moore, K. Savage, and P. Crill. 2005. A comparison of methane flux in a boreal landscape between a dry and a wet year. Global Biogeochem Cycles. 19:GB1023. doi:10.1029/2004GB002351

Carpenter, S.R., T.M. Frost, D. Heisey, and T.K. Kratz. 1989. Randomized intervention analysis and the interpretation of whole-ecosystem experiments. Ecology 70:1142–1152. doi:10.2307/1941382

Cazelles, B., M. Chavez, D. Berteaux, F. Ménard, J. Olav Vik, S. Jenouvrier, and N.C. Stenseth. 2008. Wavelet analysis of ecological time series. Oecologia 156:287–304. doi:10.1007/s00442-008-0993-2

Clymo, R.S. 1970. Growth of *Sphagnum*: Methods of measurement. J. Ecol. 58:13–49. doi:10.2307/2258168

Cottingham, K.L., J.T. Lennon, and B.L. Brown. 2005. Knowing when to draw the line: Designing more informative ecological experiments. Front. Ecol. Environ 3:145–152. doi:10.1890/1540-9295(2005)003[0145:KWTDTL]2.0.CO;2

Crill, P.M., K.B. Bartlett, R.C. Harriss, E. Gorham, E.S. Verry, D.I. Sebacher, et al. 1988. Methane flux from Minnesota peatlands. Global Biogeochem. Cycles 2:371–384.

Dietze, M.C., S.P. Serbin, C. Davidson, A.R. Desai, X.H. Feng, R. Kelly, et al. 2014. A quantitative assessment of a terrestrial biosphere model's data needs across North American biomes. J. Geophys. Res. Biogeosci. 119:286–300.

Dinsmore, K.J., M.F. Billett, U.M. Skiba, R.M. Rees, J. Drewer, and C. Helfter. 2010. Role of the aquatic pathway in the carbon and greenhouse gas budgets of a peatland catchment. Glob. Change Biol. 16:2750–2762. doi:10.1111/j.1365-2486.2009.02119.x

Dise, N., N.J. Shurpali, P. Weishampel, S.B. Verma, E.S. Verry, E. Gorham, et al. 2011. Carbon emissions from peatlands. In: R.K. Kolka, S.D. Sebestyen, E.S. Verry, and K.N. Brooks, editors, Peatland biogeochemistry and watershed hydrology at the Marcell Experimental Forest. CRC Press, Boca Raton, FL. p. 297–347.

Dorodnikov, M., M. Marushchak, C. Ciasi, and M. Wilmking. 2013. Effect of microtopography on isotopic composition of methane in porewater and efflux at a boreal peatland. Boreal Environ. Res. 18:269–279.

Fenner, N., and C. Freeman. 2011. Drought-induced carbon loss in peatlands. Nat. Geosci. 4:895–900. doi:10.1038/ngeo1323

Freeman, C., N. Fenner, N.J. Ostle, H. Kang, D.J. Dowrick, B. Reynolds, et al. 2004. Export of dissolved organic carbon from peatlands under elevated carbon dioxide levels. Nature 430:195–198. doi:10.1038/nature02707

Gorham, E. 1991. Northern peatlands: Role in the carbon cycle and probable responses to climatic warming. Ecol. Appl. 1:182–195. doi:10.2307/1941811

Gorham, E. 1995. The biogeochemistry of northern peatlands and its possible responses to global warming. In: G.M. Woodwell and F.T. MacKenzie, editors, Biotic feedbacks in the global climatic system: will the warming speed the warming? Oxford Univ. Press, Oxford, UK. p. 169–186.

Griffiths, N.A., and S.D. Sebestyen. 2016a. SPRUCE porewater chemistry data for experimental plots beginning in 2013. Carbon Dioxide Information Analysis Center, Oak Ridge National Laboratory, U.S. Department of Energy, Oak Ridge, TN. doi: http://dx.doi.org/10.3334/CDIAC/spruce.028

Griffiths, N.A., and S.D. Sebestyen. 2016b. Dynamic vertical profiles of peat porewater chemistry in a northern peatland. Wetlands 36:1119–1130. doi:10.1007/s13157-016-0829-5

Gu, L., S.G. Pallardy, K. Tu, B.E. Law, and S.D. Wullschleger. 2010. Reliable estimation of biochemical parameters from C_3 leaf photosynthesis—intercellular carbon dioxide response curves. Plant Cell Environ. 33:1852–1874. doi:10.1111/j.1365-3040.2010.02192.x

Guo, Y., R. Amundson, P. Gong, and Q. Yu. 2006. Quantity and spatial variability of soil carbon in the conterminous United States. Soil Sci. Soc. Am. J. 70:590–600. doi:10.2136/sssaj2005.0162

Hanson, P.J., A.L. Gill, X. Xu, J.R. Phillips, D.J. Weston, R.K. Kolka, et al. 2016b. Intermediate-scale community-level flux of CO_2 and CH_4 in a Minnesota peatland: Putting the SPRUCE project in a global context. Biogeochemistry 129:255–272. doi:10.1007/s10533-016-0230-8

Hanson, P.J., J.R. Phillips, J.S. Riggs, W.R. Nettles, and D.E. Todd. 2014. SPRUCE large-collar in situ CO_2 and CH_4 flux data for the SPRUCE experimental plots. Carbon Dioxide Information Analysis Center, Oak Ridge National Laboratory, U.S. Department of Energy, Oak Ridge, TN. doi:http://dx.doi.org/10.3334/CDIAC/spruce.006

Hanson, P.J., J.S. Riggs, W.R. Nettles, M.B. Krassovski, and L.A. Hook. 2015. SPRUCE deep peat heating (DPH) environmental data, February 2014 through July 2015. Carbon Dioxide Information Analysis Center, Oak Ridge National Laboratory, U.S. Department of Energy, Oak Ridge, TN. doi: http://dx.doi.org/10.3334/CDIAC/spruce.013

Hanson, P.J., J.S. Riggs, W.R. Nettles, M.B. Krassovski, and L.A. Hook. 2016a. SPRUCE whole ecosystems warming (WEW) environmental data beginning August 2015. Carbon Dioxide Information Analysis Center, Oak Ridge National Laboratory, U.S. Department of Energy, Oak Ridge, TN. doi:http://dx.doi.org/10.3334/CDIAC/spruce.032

Hanson, P.J., J.S. Riggs, W.R. Nettles, J.R. Phillips, M.B. Krassovski, L.A. Hook, et al. 2017. Attaining whole-ecosystem warming using air and deep soil heating methods with an elevated CO_2 atmosphere. Biogeosciences 14:861–883. doi:10.5194/bg-14-861-2017

Hobbie, E.A., J. Chen, P.J. Hanson, C.M. Iversen, K.J. McFarlane, N.R. Thorp, et al. 2016. Long-term carbon and nitrogen dynamics at SPRUCE revealed through stable isotopes in peat profiles. Biogeosciences Discuss. 14:2481–2494. doi:10.5194/bg-2016-261

Iversen, C.M., J. Childs, R.J. Norby, T.A. Ontl, R.K. Kolka, D.J. Brice, et al. 2017a. Fine-root growth in a forested bog is seasonally dynamic, but shallowly distributed in nutrient-poor peat. Plant Soil. doi:10.1007/s11104-017-3231-z

Iversen, C.M., J. Childs, R.J. Norby, A. Garrett, A. Martin, J. Spence, et al. 2017b. SPRUCE S1 bog fine-root production and standing crop assessed with minirhizotrons in the southern and northern ends of the S1 bog. Carbon Dioxide Information Analysis Center, Oak Ridge National Laboratory, U.S. Department of Energy, Oak Ridge, TN. doi: http://dx.doi.org/10.3334/CDIAC/spruce.019

Iversen, C.M., P.J. Hanson, D.J. Brice, J.R. Phillips, K.J. McFarlane, E.A. Hobbie, et al. 2014. SPRUCE peat physical and chemical characteristics from experimental plot cores, 2012. Carbon Dioxide Information Analysis Center, Oak Ridge National Laboratory, U.S. Department of Energy, Oak Ridge, TN. doi: http://dx.doi.org/10.3334/CDIAC/spruce.005

Iversen, C.M., J. Ledford, and R.J. Norby. 2008. CO_2 enrichment increases carbon and nitrogen input from fine roots in a deciduous forest. New Phytol. 179:837–847. doi:10.1111/j.1469-8137.2008.02516.x

Iversen, C.M., M.T. Murphy, M.F. Allen, J. Childs, D.M. Eissenstat, E.A. Lilleskov, et al. 2012. Advancing the use of minirhizotrons in wetlands. Plant Soil 352:23–39. doi:10.1007/s11104-011-0953-1

Jensen, A.M., J.M. Warren, P.J. Hanson, J. Childs, and S.D. Wullschleger. 2015a. Needle age and season influence photosynthetic temperature response in mature *Picea mariana* trees. Ann. Bot. (Lond.) 116:821–832. doi:10.1093/aob/mcv115

Jensen, A.M., J.M. Warren, P.J. Hanson, J. Childs, and S.D. Wullschleger. 2015b. SPRUCE S1 bog pretreatment photosynthesis and espiration for black spruce: 2010–2013. Carbon Dioxide Information Analysis Center, Oak Ridge National Laboratory, U.S. Department of Energy, Oak Ridge, TN. doi: http://dx.doi.org/10.3334/CDIAC/spruce.007

Koehler, A.-K., M. Sottocornola, and G. Kiely. 2011. How strong is the current carbon sequestration of an Atlantic blanket bog? Glob. Change Biol. 17:309–319. doi:10.1111/j.1365-2486.2010.02180.x

Korhola, A., J. Alm, K. Tolonen, J. Turunen, and H. Jungner. 1996. Three-dimensional reconstruction of carbon accumulation and CH_4 emission during nine millennia in a raised mire. J. Quaternary Sci. 11:161–165. doi:10.1002/(SICI)1099-1417(199603/04)11:2<161::AID-JQS248>3.0.CO;2-J

Koven, C.D., W.J. Riley, Z.M. Subin, J.Y. Tang, M.S. Torn, W.D. Collins, et al. 2013. The effect of vertically resolved soil biogeochemistry and alternate soil C and N models on C dynamics of CLM4. Biogeosciences 10:7109–7131. doi:10.5194/bg-10-7109-2013

Krassovski, M.B., J.S. Riggs, L.A. Hook, W.R. Nettles, P.J. Hanson, and T.A. Boden. 2015. A comprehensive data acquisition and management system for an ecosystem-scale peatland warming and elevated CO_2 experiment. Geosci. Instrum. Method. Data Syst. 4:203–213. doi:10.5194/gi-4-203-2015

Lafleur, P.M., N.T. Roulet, J.L. Bubier, S. Frolking, and T.R. Moore. 2003. Interannual variability in the peatland-atmosphere carbon dioxide exchange at an ombrotrophic bog. Global Biogeochem. Cycles 17:1036.

doi:10.1029/2002GB001983

Limpens, J., F. Berendse, C. Blodau, J.G. Canadell, C. Freeman, J. Holden, et al. 2008. Peatlands and the carbon cycle: From local processes to global implications—a synthesis. Biogeosciences 5:1475–1491. doi:10.5194/bg-5-1475-2008

Loisel, J., Z. Yu, D.W. Beilman, P. Camill, J. Alm, M.J. Amesbury, et al. 2014. A database and synthesis of northern peatland soil properties and Holocene carbon and nitrogen accumulation. Holocene 24:1028–1042. doi:10.1177/0959683614538073

Lu, X.J., Y.P. Wang, T. Ziehn, and Y.J. Dai. 2014. An efficient method for global parameter sensitivity analysis and its applications to the Australian community land surface model (CABLE). Agric. For. Meteorol. 182:292–303. doi:10.1016/j.agrformet.2013.04.003

Mao, J., D.M. Ricciuto, P.E. Thornton, J.M. Warren, A.W. King, X. Shi, et al. 2016. Evaluating the Community Land Model in a pine stand with shading manipulations and $^{13}CO_2$ labeling. Biogeosciences 13:641–657. doi:10.5194/bg-13-641-2016

Melton, J.R., R. Wania, E.L. Hodson, B. Poulter, B. Ringeval, R. Spahni, et al. 2013. Present state of global wetland extent and wetland methane modelling: Conclusions from a model inter-comparison project (WETCHIMP). Biogeosciences 10:753–788. doi:10.5194/bg-10-753-2013

Moore, T.R., N.T. Roulet, and J.M. Waddington. 1998. Uncertainty in predicting the effect of climatic change on the carbon cycling of Canadian peatlands. Clim. Change 40:229–245. doi:10.1023/A:1005408719297

Nilsson, M., J. Sagerfors, I. Buffam, H. Laudon, T. Eriksson, A. Grelle, et al. 2008. Contemporary carbon accumulation in a boreal oligotrophic minerogenic mire—a significant sink after accounting for all C-fluxes. Glob. Change Biol. 14:2317–2332. doi:10.1111/j.1365-2486.2008.01654.x

Norby, R.J., J.S. Hartz-Rubin, and M.J. Verbrugge. 2003. Phenological responses in maple to experimental atmospheric warming and CO_2 enrichment. Glob. Change Biol. 9:1792–1801. doi:10.1111/j.1365-2486.2003.00714.x

Ohlson, M., and R.H. Økland. 1998. Spatial variation in rates of carbon and nitrogen accumulation in a boreal bog. Ecology 79:2745–2758. doi:10.1890/0012-9658(1998)079[2745:SVIROC]2.0.CO;2

Olefeldt, D., N.T. Roulet, O. Bergeron, P. Crill, K. Bäckstrand, and T.R. Christensen. 2012. Net carbon accumulation of a high-latitude permafrost palsa mire similar to permafrost-free peatlands. Geophys. Res. Lett. 39:L03501. doi:10.1029/2011GL050355

Oleson, K.W., D.M. Lawrence, G.B. Bonan, B. Drewniak, M. Huang, C.D. Koven et al. 2013. Technical description of version 4.5 of the Community Land Model (CLM). NCAR Technical Note NCAR/TN-503+STR. National Center for Atmospheric Research, Boulder, CO.

Parsekian, A.D., L. Slater, D. Ntarlagiannis, J. Nolan, S.D. Sebestyen, R.K. Kolka, et al. 2012. Uncertainty in peat volume and soil carbon estimated using ground-penetrating radar and probing. Soil Sci. Soc. Am. J. 76:1911–1918. doi:10.2136/sssaj2012.0040

Phillips, J.R., D.J. Brice, P.J. Hanson, J. Childs, C.M. Iversen, R.J. Norby, et al. 2017. SPRUCE pretreatment plant tissue analyses, 2009 through 2013. Carbon Dioxide Information Analysis Center, Oak Ridge National Laboratory, U.S. Department of Energy, Oak Ridge, TN. doi: http://dx.doi.org/10.3334/CDIAC/spruce.038

Piao, S., P. Friedlingstein, P. Ciais, N. Viovy, and J. Demarty. 2007. Growing season extension and its impact on terrestrial carbon cycle in the Northern Hemisphere over the past 2 decades. Global Biogeochem Cycles. 21:GB3018. doi:10.1029/2006GB002888

Richardson, A.D., T.F. Kennan, M. Migliavacca, Y. Ryu, O. Sonnentag, and M. Toomey. 2013. Climate change, phenology, and phenological control of vegetation feedbacks to the climate system. Agric. For. Meteorol. 169:156–173. doi:10.1016/j.agrformet.2012.09.012

Roulet, N.T., P.M. Lafleur, P.J.H. Richard, T.R. Moore, E.R. Humphreys, and J. Bubier. 2007. Contemporary carbon balance and late Holocene carbon accumulation in a northern peatland. Glob. Change Biol. 13:397–411.

Roulet, N., T. Moore, J. Bubier, and P. Lafleur. 1992. Northern fens: Methane flux and climatic change. Tellus 44:100–105. doi:10.3402/tellusb.v44i2.15429

Rydin, H., and J.K. Jeglum. 2013. The biology of peatlands. 2nd ed. Oxford Univ. Press, Oxford, UK.

Saltelli, A., S. Tarantola, F. Campolongo, and M. Ratto. 2004. Sensitivity analysis in practice: A guide to assessing scientific models. John Wiley & Sons Inc., Hoboken, NJ.

Sargsyan, K., C. Safta, H.N. Najm, B.J. Debusschere, D. Ricciuto, and P. Thornton. 2014. Dimensionality reduction for complex models via Bayesian compressive sensing. Int. J. Uncertain. Quantif. 4:63–93. doi:10.1615/Int.J.UncertaintyQuantification.2013006821

Sebestyen, S.D., C. Dorrance, D.M. Olson, E.S. Verry, R.K. Kolka, A.E. Elling, et al. 2011a. Long-term monitoring sites and trends at the Marcell Experimental Forest. In: R.K. Kolka, S.D. Sebestyen, E.S. Verry, and K.N. Brooks, editors, Peatland biogeochemistry and watershed hydrology at the Marcell Experimental Forest. CRC Press, Boca Raton, FL. p. 15–71.

Sebestyen, S.D., and N.A. Griffiths. 2016. SPRUCE enclosure corral and sump system: Description, operation, and calibration. Climate Change Science Institute, Oak Ridge National Laboratory, U.S. Department of Energy, Oak Ridge, TN. doi: http://dx.doi.org/10.3334/CDIAC/spruce.030

Sebestyen, S.D., and E.S. Verry. 2011. Effects of watershed experiments on water chemistry at the Marcell Experimental Forest. In: R.K. Kolka, S.D. Sebestyen, E.S. Verry, and K.N. Brooks, editors, Peatland biogeochemistry and watershed hydrology at the Marcell Experimental Forest. CRC Press, Boca Raton, FL. p. 433–458.

Sebestyen, S.D., E.S. Verry, and K.N. Brooks. 2011b. Hydrological responses to forest cover changes on uplands and peatlands. In: R.K. Kolka, S.D. Sebestyen, E.S. Verry, and K.N. Brooks, editors, Peatland biogeochemistry and watershed hydrology at the Marcell Experimental Forest. CRC Press, Boca Raton, FL. p. 401–432.

Shi, X., P.E. Thornton, D.M. Ricciuto, P.J. Hanson, J. Mao, S.D. Sebestyen, et al. 2015. Representing northern peatland microtopography and hydrology within the Community Land Model. Biogeosciences 12:6463–6477. doi:10.5194/bg-12-6463-2015

Shurpali, N.J., S.B. Verma, and J. Kim. 1995. Carbon dioxide exchange in a peatland ecosystem. J. Geophys. Res. 100:14319–14326. doi:10.1029/95JD01227

Sobol, I.M. 1993. Sensitivity estimates for nonlinear mathematical models. Math. Model. Comput. Exp. 1:407–414.

Stewart-Oaten, A., W.W. Murdoch, and K.R. Parker. 1986. Environmental impact assessment: "pseudoreplication" in time? Ecology 67:929–940. doi:10.2307/1939815

Strack, M., J.M. Waddington, and E.-S. Tuittila. 2004. Effect of water table drawdown on northern peatland methane dynamics: Implications for climate change. Global Biogeochem Cycles. 18:GB4003.

Stuiver, M., and H.A. Polach. 1977. Reporting of ^{14}C data. Radiocarbon 19:355–363. doi:10.1017/S0033822200003672

Sulman, B.N., A.R. Desai, N.M. Schroeder, D. Ricciuto, A. Barr, A.D. Richardson, et al. 2012. Impact of hydrological variations on modeling of peatland CO_2 fluxes: Results from the North American Carbon Program site synthesis. J. Geophys. Res. Biogeosci. 117:G0103. doi:10.1029/2011JG001862

Thornton, P.E., and N.A. Rosenbloom. 2005. Ecosystem model spin-up: Estimating steady state conditions in a coupled terrestrial carbon and nitrogen cycle model. Ecol. Model. 189:25–48. doi:10.1016/j.ecolmodel.2005.04.008

Tian, H.Q., C.Q. Lu, J. Yang, K. Banger, D.N. Huntzinger, C.R. Schwalm, et al. 2015. Global patterns and controls of soil organic carbon dynamics as simulated by multiple terrestrial biosphere models: Current status and future directions. Global Biogeochem. Cycles 29:775–792. doi:10.1002/2014GB005021

Turunen, J., E. Tomppo, K. Tolonen, and A. Reinikainen. 2002. Estimating carbon accumulation rates of undrained mires in Finland: Application to boreal and subarctic. Holocene 12:69–80. doi:10.1191/0959683602hl522rp

Underwood, A.J. 1994. On beyond BACI: Sampling designs that might reliably detect environmental disturbances. Ecol. Appl. 4:3–15. doi:10.2307/1942110

van Bellen, S., P.-L. Dallaire, M. Garneau, and Y. Bergeron. 2011. Quantifying spatial and temporal Holocene carbon accumulation in ombrotrophic peatlands of the Eastmain region, Quebec, Canada. Global Biogeochem Cycles. 35:GB2016.

Verry, E.S., K.N. Brooks, D.S. Nichols, D.R. Ferris, and S.D. Sebestyen. 2011. Watershed hydrology. In: R.K. Kolka, S.D. Sebestyen, E.S. Verry, and K.N. Brooks, editors, Peatland biogeochemistry and watershed hydrology at the Marcell Experimental Forest. CRC Press, Boca Raton, FL. p. 193–212.

Vogel, J.S., J.R. Southon, D.E. Nelson, and T.A. Brown. 1984. Performance of catalytically condensed carbon for use in accelerator mass spectrometry. Nucl. Instrum. Meth. Phys Res. B 5:289–293. doi:10.1016/0168-583X(84)90529-9

Waddington, J.M., and N.T. Roulet. 1996. Atmosphere–wetland carbon exchanges: Scale dependency of CO_2 and CH_4 exchange on the developmental topography of a peatland. Global Biogeochem. Cycles 10:233–245. doi:10.1029/95GB03871

Waddington, J.M., and N.T. Roulet. 2000. Carbon balance of a boreal patterned peatland. Glob. Change Biol. 6:87–97. doi:10.1046/j.1365-2486.2000.00283.x

Walker, A.P., K.R. Carter, L. Gu, P.J. Hanson, A. Malhotra, R.J. Norby, et al. 2017. Biophysical drivers of seasonal variability in *Sphagnum* gross primary production in a northern temperate bog. J. Geophys. Res. Biogeosci. 122. doi:10.1002/2016JG003711

White, M.A., P.E. Thornton, S.W. Running, and R.R. Nemani. 2000. Parameterization and sensitivity analysis of the Biome-BGC terrestrial ecosystem model: Net primary production controls. Earth Interact. 4:1–85. doi:10.1175/1087-3562(2000)004<0003:PASAOT>2.0.CO;2.

Wilson, R.M., A.M. Hopple, M.M. Tfaily, S.D. Sebestyen, C.W. Schadt, L. Pfeifer-Meister, et al. 2016. Stability of a peatland carbon bank to rising temperatures. Nat. Commun. 7:13723. doi:10.1038/ncomms13723

Wu, J., and N.T. Roulet. 2014. Climate change reduces the capacity of northern peatlands to absorb the atmospheric carbon dioxide: The different responses of bogs and fens. Global Biogeochem. Cycles 28:1005–1024. doi:10.1002/2014GB004845

Xu, X.F., D.A. Elias, D.E. Graham, T.J. Phelps, S.L. Carroll, S.D. Wullschleger, and P.E. Thornton. 2015. A microbial functional group-based module for simulating methane production and consumption: Application to an incubated permafrost soil. J. Geophys. Res. Biogeosci. 120:1315–1333. doi:10.1002/2015JG002935

Yanai, R.D., C.R. Levine, M.B. Green, and J.L. Campbell. 2012. Quantifying uncertainty in forest nutrient budgets. J. For. 110:448–456.

Yu, Z.C. 2012. Northern peatland carbon stocks and dynamics: A review. Biogeosciences 9:4071–4085. doi:10.5194/bg-9-4071-2012

Yu, Z.C., J. Loisel, D.P. Brosseau, D.W. Beilman, and S.J. Hunt. 2010. Global peatland dynamics since the Last Glacial Maximum. Geophys. Res. Lett. 37:L13402. doi:10.1029/2010GL043584

Supplementary Material

Table S1. List of environmental and ecosystem process measurements collected in the S1 bog, the methodology used to collect these measurements, and the temporal and spatial scale at which the data were collected and presented. "Plots" represents measurements that were collected within the all or a subset of the 17 SPRUCE plots (see Fig. 1), "subplots" represents measurements that were collected at multiple sampling locations within a "plot", and "outside the plots" represents measurements that were collected outside the plot locations, either in between plots or south or north of the 3 transect boardwalks (see Fig. 1).

Measurement	Methodology	Temporal scale	Spatial scale
Air Temperature, °C	Thermistors	Half-hourly (2014–2016)	4 plots (#s 5, 7, 14, 21)
Soil temperature, °C	Multipoint thermistor probes	Half-hourly (2014–2016)	4 plots (#s 5, 7, 14, 21)
[CO_2], ppm	Sampling manifold attached to a LiCor LI-840	6-minute (2015–2016)	4 plots (#s 5, 7, 14, 21)
Soil water, cm^3 cm^{-3}	Soil moisture probes (10HS Decagon Devices Inc.)	Monthly (summer 2015)	27-28 Subplots (n = 2–3 locations in each of 10 plots: 4, 6, 8, 10, 11, 13, 16, 17, 19, 20)
Peat depth, m	Segmented peat push probe	N/A	17 plots (#s 2, 4, 5, 6, 7, 8, 9, 10, 11, 13, 14, 15, 16, 17, 19, 20, 21)
Phenology	Visual and camera observations	Annually (2010–2015)	N/A
Tree NPP, g C m^{-2} y^{-1}	Tree basal area and height measurements converted to dry mass using an allometric equation	Annually (2011–2015)	12 plots (#s 4, 6, 7, 8, 10, 11, 13, 16, 17, 19, 20, 21)
Shrub NPP, g C m^{-2} y^{-1}	Annual destructive harvests	Annually (2012–2015)	17 plots (#s 2, 4, 5, 6, 7, 8, 9, 10, 11, 13, 14, 15, 16, 17, 19, 20, 21)
Sphagnum NPP, g C m^{-2} y^{-1}	Brush wires and *Sphagnum* bundles	Annually (2012–2015)	12 plots (#s 4, 6, 7, 8, 10, 11, 13, 16, 17, 19, 20, 21)
Sphagnum and peat NEE, µmol m^{-2} d^{-1}	LI-COR 8100-104C 20-cm diameter chambers	Daily (June–Nov. 2014)	Outside the plots (n = 6 locations)
Foliar respiration (shrubs), µmol m^{-2} s^{-1}	Gas exchange rates using Li-6400	Seasonally (2010–2015)	Outside the plots (n = 10–11 locations)
Foliar respiration (trees), µmol m^{-2} s^{-1}	Gas exchange rates using Li-6400	Seasonally (2010–2015)	Outside the plots (n = 6–8 locations)
Photosynthesis at light saturation (shrubs), µmol m^{-2} s^{-1}	Gas exchange rates using Li-6400	Seasonally (2010–2015)	Outside the plots (n = 11 locations)
Photosynthesis at light saturation (trees), µmol m^{-2} s^{-1}	Gas exchange rates using Li-6400	Seasonally (2010–2015)	Outside the plots (n = 6–8 locations)
Heterotrophic CO_2 efflux, µmol m^{-2} s^{-1}	CO_2 open-path analyzer over a 1.13 m^2 area	Monthly (during the growing season) (2013–2015)	10 plots (#s 4, 6, 8, 10, 11, 13, 16, 17, 19, 20)
Net CH_4 efflux, µmol m^{-2} s^{-1}	CH_4 open-path analyzer over a 1.13 m^2 area	Monthly (during the growing season) (2013–2015)	10 plots (#s 4, 6, 8, 10, 11, 13, 16, 17, 19, 20)
Fine-root biomass production (trees), [proportion of annual max for temporal; g C m^{-2} y^{-1} for spatial]	Minirhizotrons	Weekly (during the growing season) (2011–2012)	Outside the plots (n = 24 locations)
Fine-root biomass production (shrubs), [proportion of annual max for temporal; g C m^{-2} y^{-1} for spatial]	Minirhizotrons	Weekly (during the growing season) (2011–2012)	Outside the plots (n = 24 locations)

Fine-root peak standing crop (trees), g C m^{-2}	Minirhizotrons	N/A	Outside the plots (n = 24 locations)
Fine-root peak standing crop (shrubs), g C m^{-2}	Minirhizotrons	N/A	Outside the plots (n = 24 locations)
TOC yield, g C m^{-2} y^{-1}	Piezometer for porewater collection and subsurface corral for lateral outflow	N/A	10 plots (#s 4, 6, 8, 10, 11, 13, 16, 17, 19, 20)
Peat chemistry	Peat cores and chemical analyses	N/A	16 plots (#s 4, 5, 6, 7, 8, 9, 10, 11, 13, 14, 15, 16, 17, 19, 20, 21)
Porewater TOC, g C/L	Piezometer for porewater collection and chemical analyses	N/A	16 plots (#s 4, 5, 6, 7, 8, 9, 10, 11, 13, 14, 15, 16, 17, 19, 20, 21)
Fine-root biomass density, g C m^{-3}	Root ingrowth cores	N/A	Outside the plots (n = 12 locations)